DETECÇÃO REMOTA MULTIESPETRAL

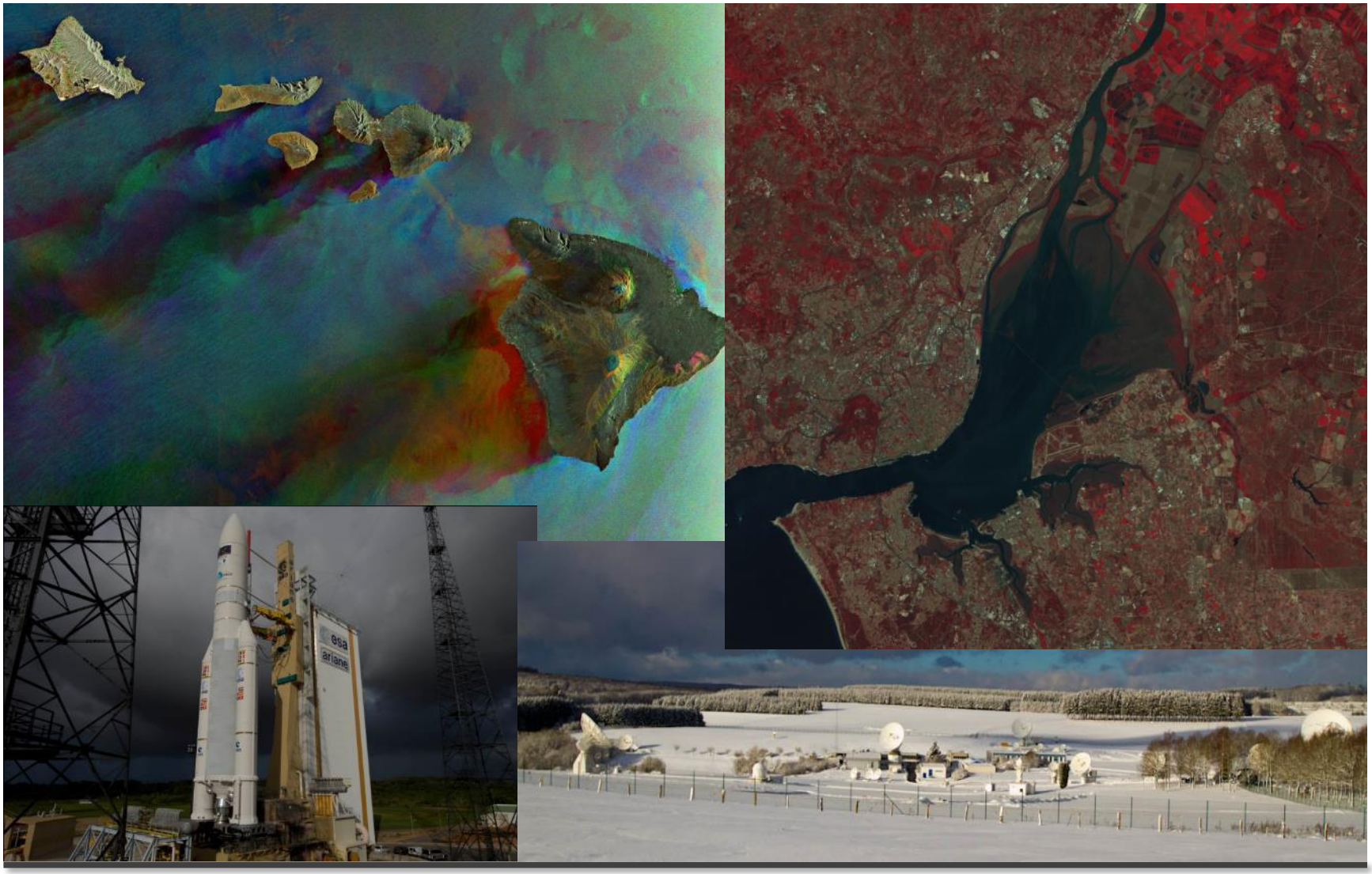

DETECÇÃO REMOTA MULTIESPETRAL

Programa -Teórica

Cap. 1 A Detecção Remota

Cap. 2 Princípios Físicos da Deteção Remota

Cap. 3 Satélites e Sensores

Cap. 4 Classificação de Imagem

Cap. 5 Aprendizagem Automática

DETECÇÃO REMOTA MULTIESPETRAL

Capitulo 1 – A Detecção Remota

- O que é da Detecção Remota
- Radiação Electromagnética
- Interacção com atmosfera
- Interacção Radiação-Alvo
- Assinatura Espectral
- Detecção Passiva vs Activa
- Sensores Ópticos
- Características das imagens
- Resolução Espacial, Espectral, Radiométrica e Temporal
- Formato dos dados
- Sistemas de imagens

DETECÇÃO REMOTA MULTIESPETRAL

Capitulo 2 – Princípios Físicos da Detecção Remota

- Características da radiação eletromagnética
- Equações de Maxwell
- Quantidades radiométricas
- Interação da radiação com a matéria
- Radiação Térmica
- Fontes de radiação eletromagnética
- Radiação Solar
- Interação com a atmosfera
- Conversão DN para radiância
- Correcção radiométrica e Geométrica de imagens

DETECÇÃO REMOTA MULTIESPETRAL

Capitulo 3 – Satélites e Sensores

- Satélites Meteorológicos
  - GOES, NOAA AVHRR, Outros satélites
- Satélites de Observação do Mar
- Altimetria Espacial
- Missões Geopotenciais Espaciais
- Missões na banda do visível
  - LANSAT, SPOT, IRS, IKONOS, QuickBird, GeoEye-1

DETECÇÃO REMOTA MULTIESPETRAL

Capitulo 4 – Classificação de Imagens Multiespetrais

- Índices (empíricos) de Vegetação
- Classificação de Imagem
  - Unsupervised (K-Means, ISODATA)
  - Supervised
    - Classificação de Máxima Verosimilhança
    - Classificador Distância mínima
    - Classificador Paralelepípedo
    - Classificador Mahalanobis
- Avaliação da precisão da classificação

Capitulo 5 – Aprendizagem Automática

- Aprendizagem automática (Machine Learning)
- Classificação binária
- Conceito de aprendizagem
- Modelos em árvore (decision tree, random forest)
- Modelos lineares (Perceptron, SVM)
- Modelos baseados na distancia (NN, Kmeans)
- Redes Neurais Convolucionais (CNN)

DETECÇÃO REMOTA MULTIESPETRAL

Avaliação / assessment

Exame Escrito	50%
Apresentação e discussão de um artigo científico	10%
Relatório do trabalho prático:	40%

A data limite para entrega do trabalho prático é **27 março de 2025.**
Haverá uma apresentação oral do trabalho no dia **28 de março 2025**.

DETECÇÃO REMOTA MULTIESPETRAL

Trabalho Prático

Realização de um projecto de detecção remota (a ser definido)

Artigo Cientifico

Artigo sobre o uso de inteligência artificial na classificação de imagem.
Keywords: Machine learning, Deep learning, Neural networks, CNN

DETECÇÃO REMOTA MULTIESPETRAL

Calendarização das aulas Teóricas

Data	Descrição
18 Fev.	Apresentação da Disciplina. Avaliação.
19 Fev.	A Deteção Remota
19 Fev.	A Deteção Remota. (Assinatura Espectral, Formato dos dados)
25 Fev.	Princípios Físicos da Deteção Remota (até interação atmosfera)
26 Fev.	Princípios Físicos da Deteção Remota (exercícios)
26 Fev.	Satélites e Sensores: Satélites Meteorológicos: GOES, NOAA AVHRR, Outros satélites, Altimetria Espacial, Missões Geopotenciais Espaciais
11 Mar.	Satélites e Sensores: Observação da Terra
12 Mar.	Classificação Imagem
12 Mar.	Classificação Imagem
18 Mar.	Classificação Imagem (exercícios)
19 Mar.	Aprendizagem automática
19 Mar.	Apresentação pelos alunos de um artigo científico

DETECÇÃO REMOTA MULTIESPETRAL

Bibliografia

- Fundamentals of Remote Sensing, Canada Centre for Remote Sensing. http://www.ccrs.nrcan.gc.ca/resource/tutor/fundam/index_e.php

- Ana Duarte Fonseca, João Cordeiro Fernandes, "Detecção Remota". LIDEL.

- R.A. Schowengerdt, "Remote Sensing. Models and Methods for Image Processing", Academic Press ed.

- Remote Sensing Digital Image Analysis, An Introduction. Hohn A. Richards. Springer-Verlag.

- Principles and Applications of Imaging Radar. Manual of Remote Sensing, Third Edition, Vol. 2. Edited by Floyd M. Henderson and Anthony J. Lewis.

- Remote Sensing of the Earth Sciences. Manual of Remote Sensing, Third Edition, Vol. 3. Edited by Andrew N. Rencz.

DETECÇÃO REMOTA MULTIESPETRAL

Agencias Espaciais

www.esa.int	European Space Agency
www.nasa.gov	National Aeronautics and Space Administration
www.dlr.de	Deutches Zentrum für Luft- und Raumfahrt
www.nasda.go.jp	National Space Development Agency of Japan
www.cnes.fr	Centre National d'études Spatiales
www.space.gc.ca	Canadian Space Agency
www.bnsc.gov.uk	British National Space Centre
www.isro.org	Indian Space Research Organization

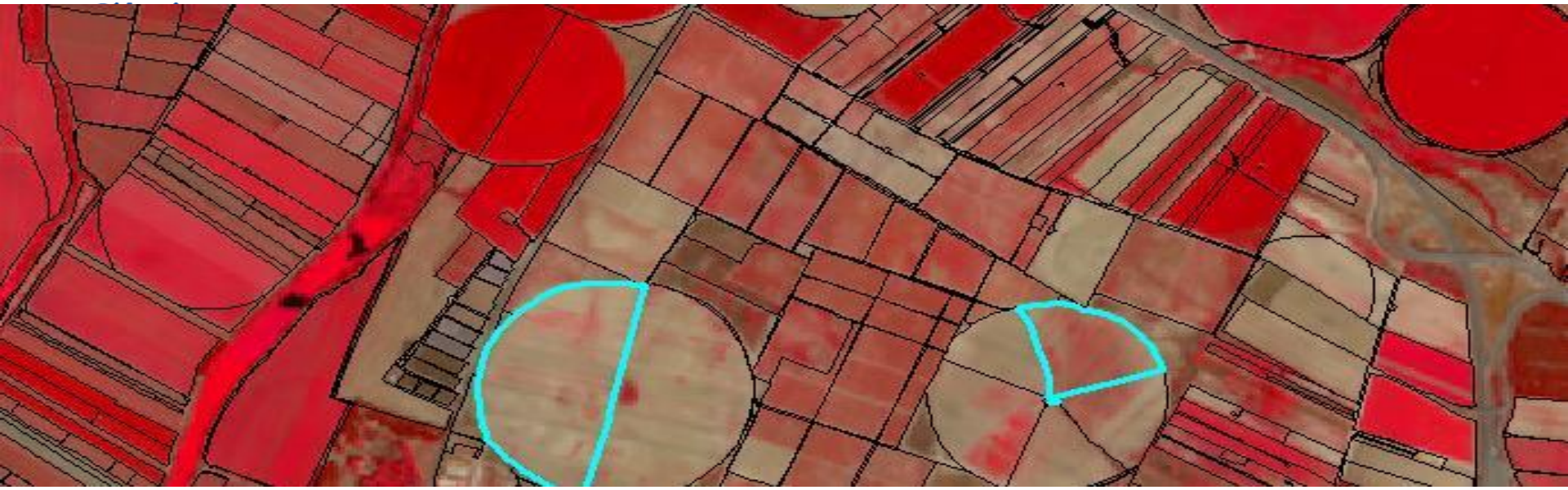

Apoio à implementação de um sistema de alerta para monitorização da atividade agrícola com base em imagem de satélite e inteligência artificial

João Catalão, Ana Navarro

IDL, Faculty of Sciences, University of Lisbon, Portugal;

Ciências ULisboa

CAP, Common Agriculture Policy

Objectivos

- Estudo de marcadores fenológicos de culturas agrícolas relevantes em termos da monitorização da ocupação do solo;

- Desenvolvimento de uma metodologia que valide a candidatura do agricultor em termos da sua conformidade, e não conformidade ou dúvida;

- Prototipagem do sistema de implementação do modelo;

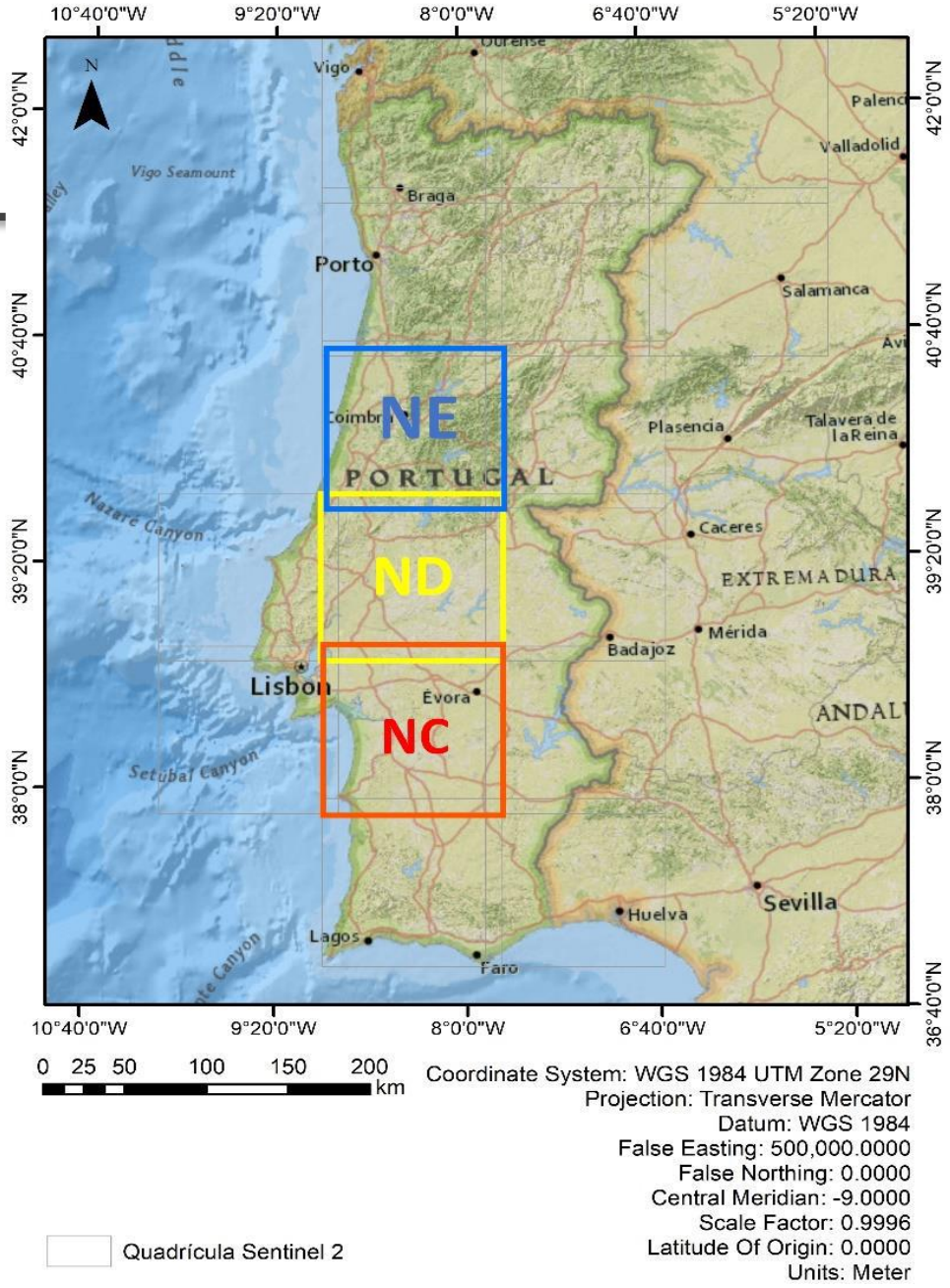
10°40'0"W
9°20'0"W
8°0'0"W
6°40'0"W
5°20'0"W
42°0'0"N
40°40'0"N
39°20'0"N
38°0'0"N
36°40'0"N
N
Vigo
Ourense
Palencia
Valladolid
Vigo Seamount
Braga
Porto
Salamanca
Avila
Coimbra
NE
PORTUGAL
Plasencia
Talavera de la Reina
Nazaré Canyon
ND
Caceres
EXTREMADURA
Mérida
Badajoz
Lisbon
Évora
NC
ANDALUCIA
Setubal Canyon
Sevilla
Huelva
Lagos
Faro
0 25 50 100 150 200
km
Coordinate System: WGS 1984 UTM Zone 29N
Projection: Transverse Mercator
Datum: WGS 1984
False Easting: 500,000.0000
False Northing: 0.0000
Central Meridian: -9.0000
Scale Factor: 0.9996
Latitude Of Origin: 0.0000
Units: Meter
Quadrícula Sentinel 2

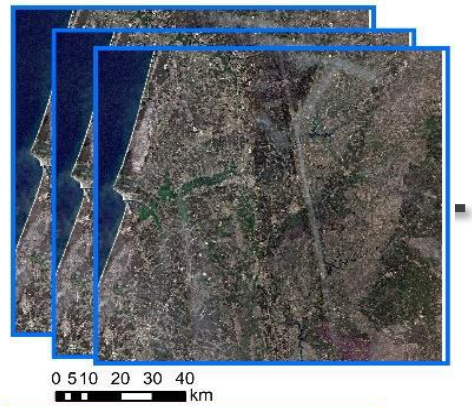
0 5 10 20 30 40
km

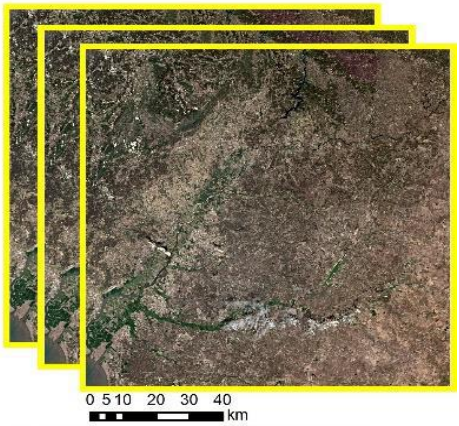
0 5 10 20 30 40
km

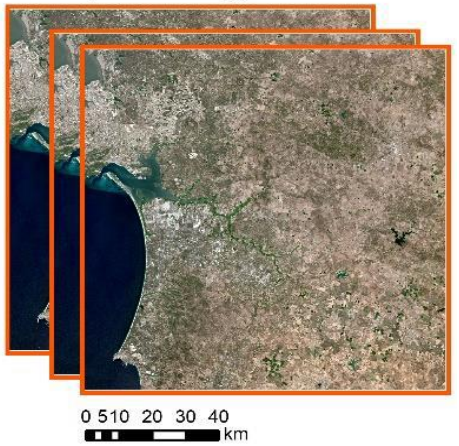
0 5 10 20 30 40
km

Distribuição do tipo de culturas por região/ano.

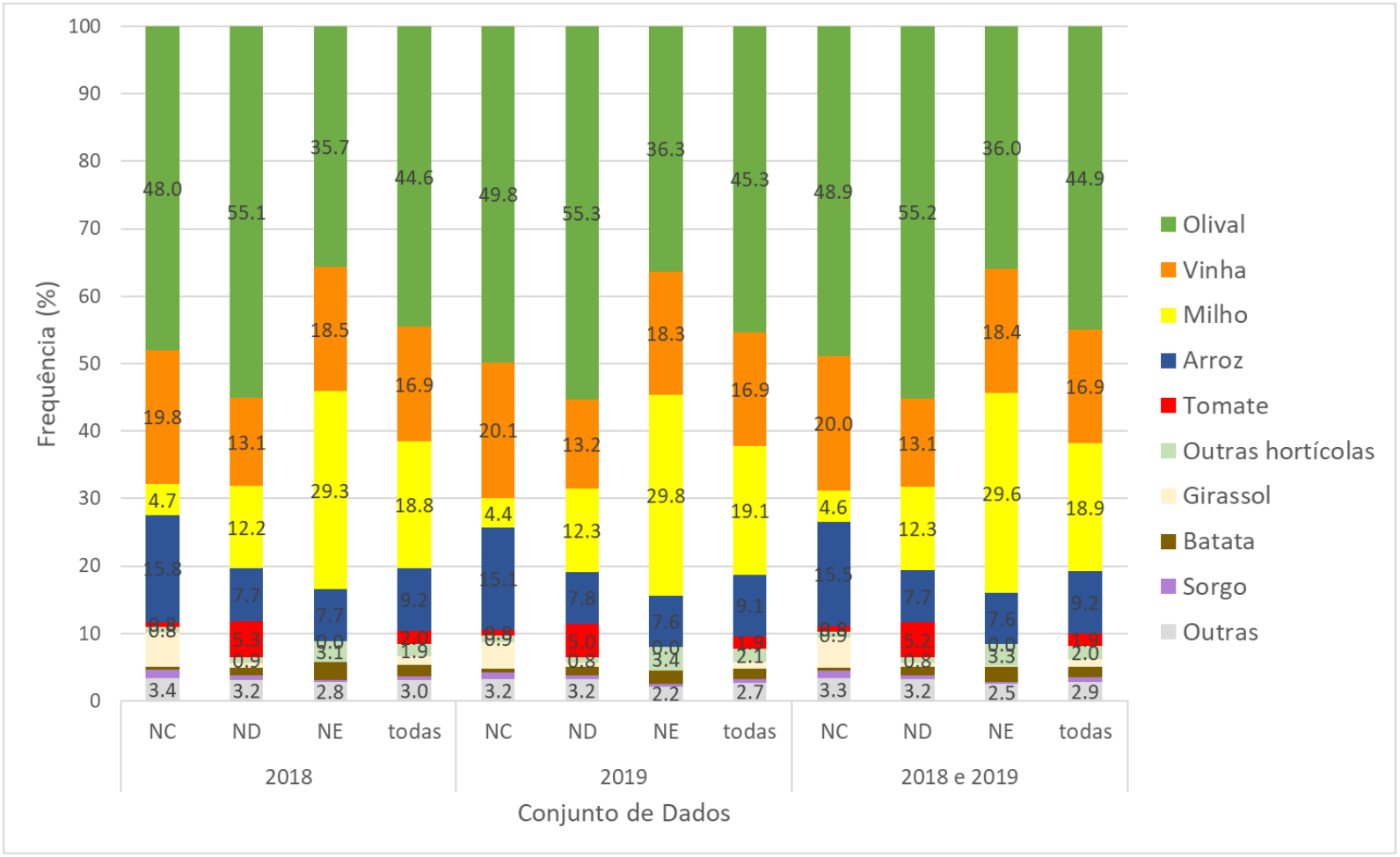

Imagens Sentinel-2 e parcelas

Ano	Zona	Março		Abril			Maio					Junho				Julho				Agosto						Setembro					Outubro	
		21	26	20	25	30	05	10	15	25	30	09	19	24	29	14	19	24	29	03	08	13	18	23	28	02	07	12	22	27	07	12
2018	NE																															
	ND																															
	NC																															
2019	NE																															
	ND																															
	NC																															

Nome do conjunto de dados (ano, zona geográfica)	N.º de parcelas (amostras)	N.º de variáveis	N.º de Imagens
2018 NE	62335	108	12
2018 ND	44795	90	10
2018 NC	25137	117	13
2019 NE	61980	126	14
2019 ND	44563	162	18
2019 NC	25137	153	17

DESAFIOS /PROBLEMAS

Controlo da atividade agrícola (atividade vegetativa)

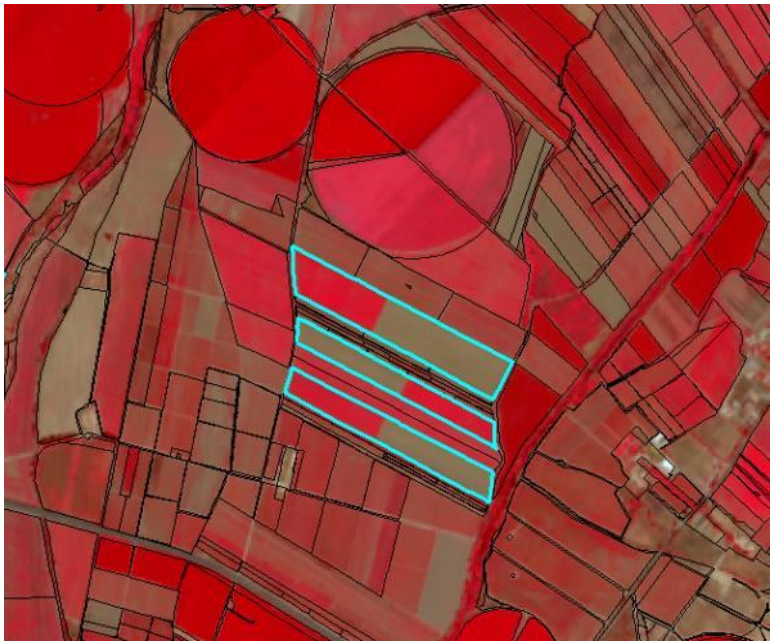

Declarada como Tomate

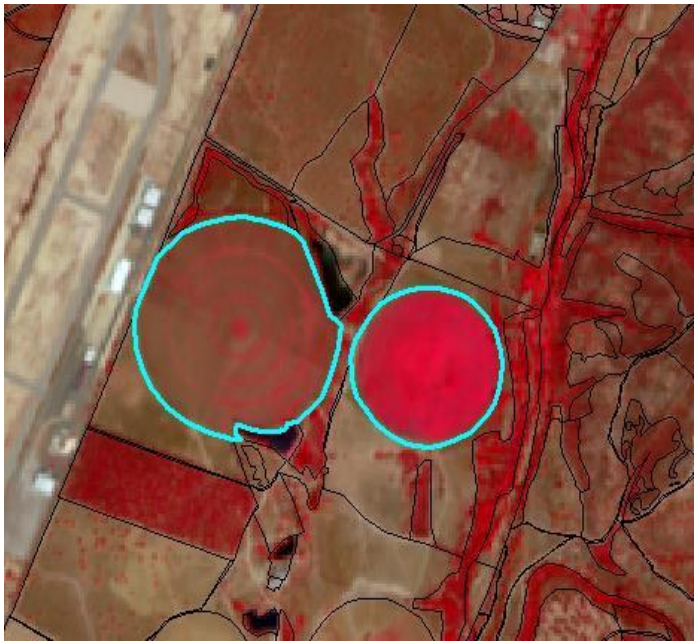

Declarada como pastagem permanente (permanent pasture)

Controlo da atividade agrícola (atividade vegetativa)

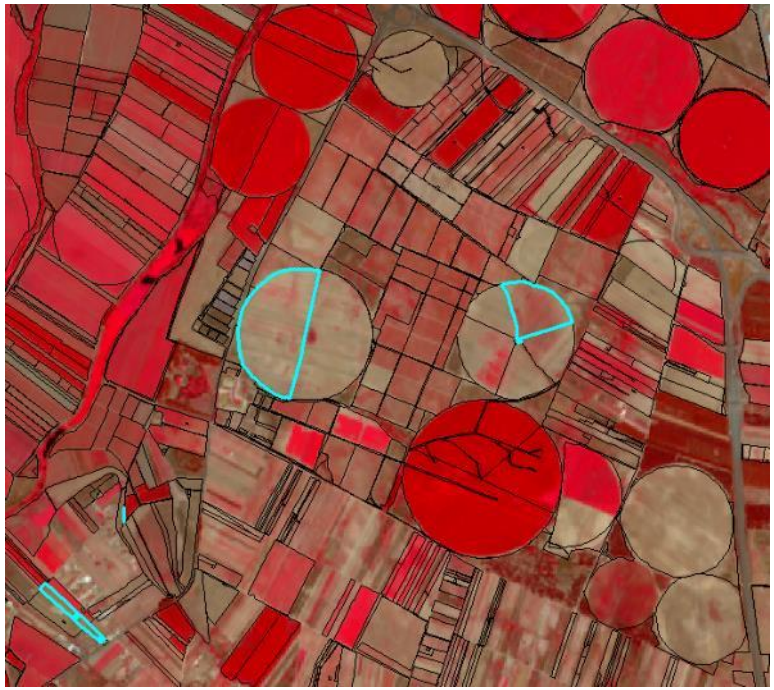

declaradas como Milho (Corn)	Declarado como Milho

Transfer Learning / Transferencia da Aprendizagem

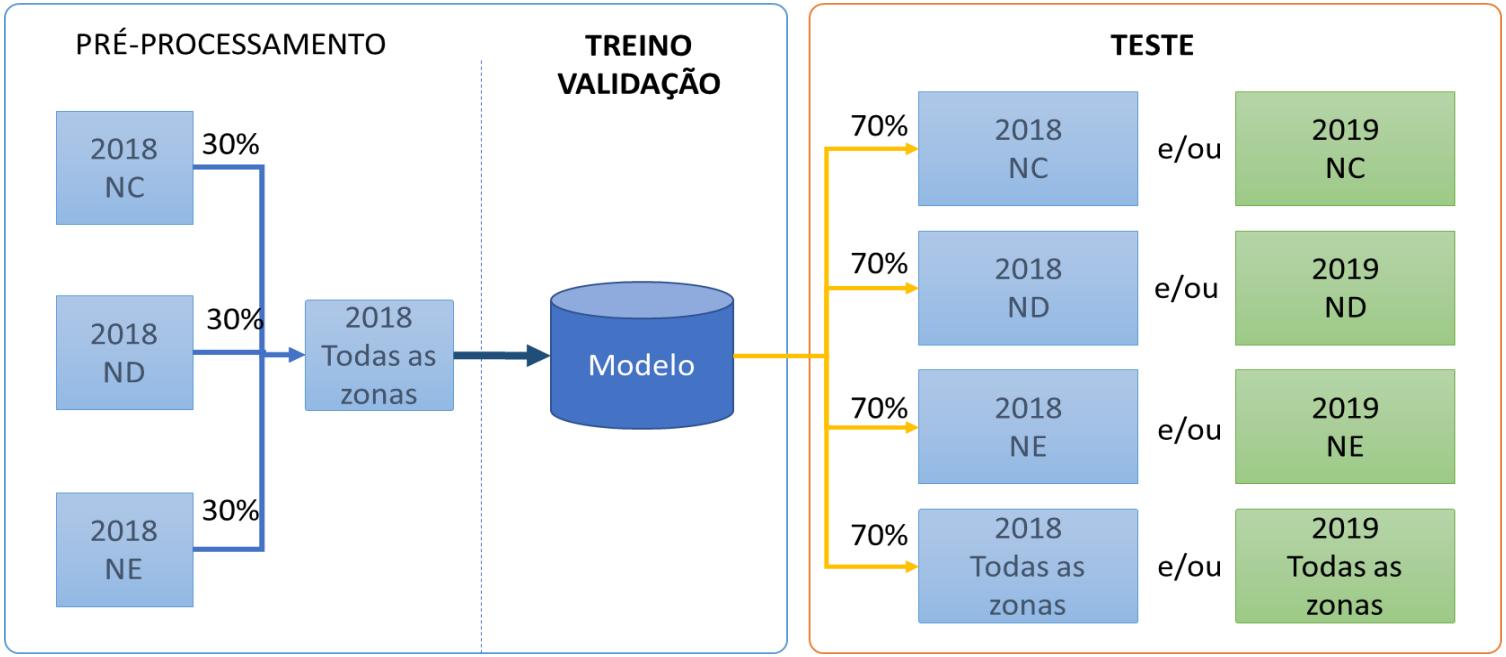

As declarações dos agricultores são usadas para treino do classificador

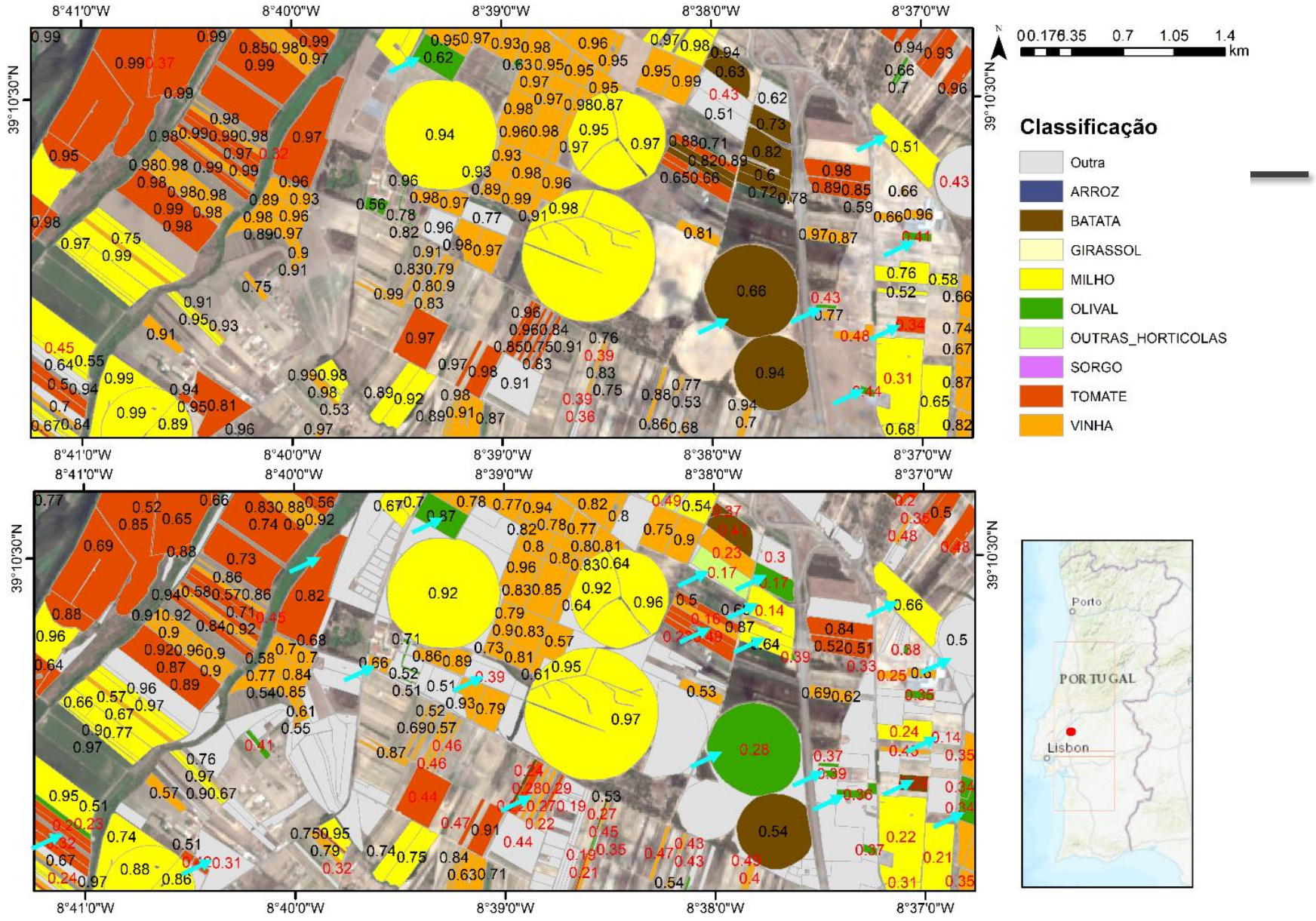

Mapa de confiança (2019 zona ND) para as mesmas parcelas e para modelo sem TL (T02, em cima) e com TL no tempo (T06, em baixo) (o apontador azul indica parcelas incorretamente classificadas).

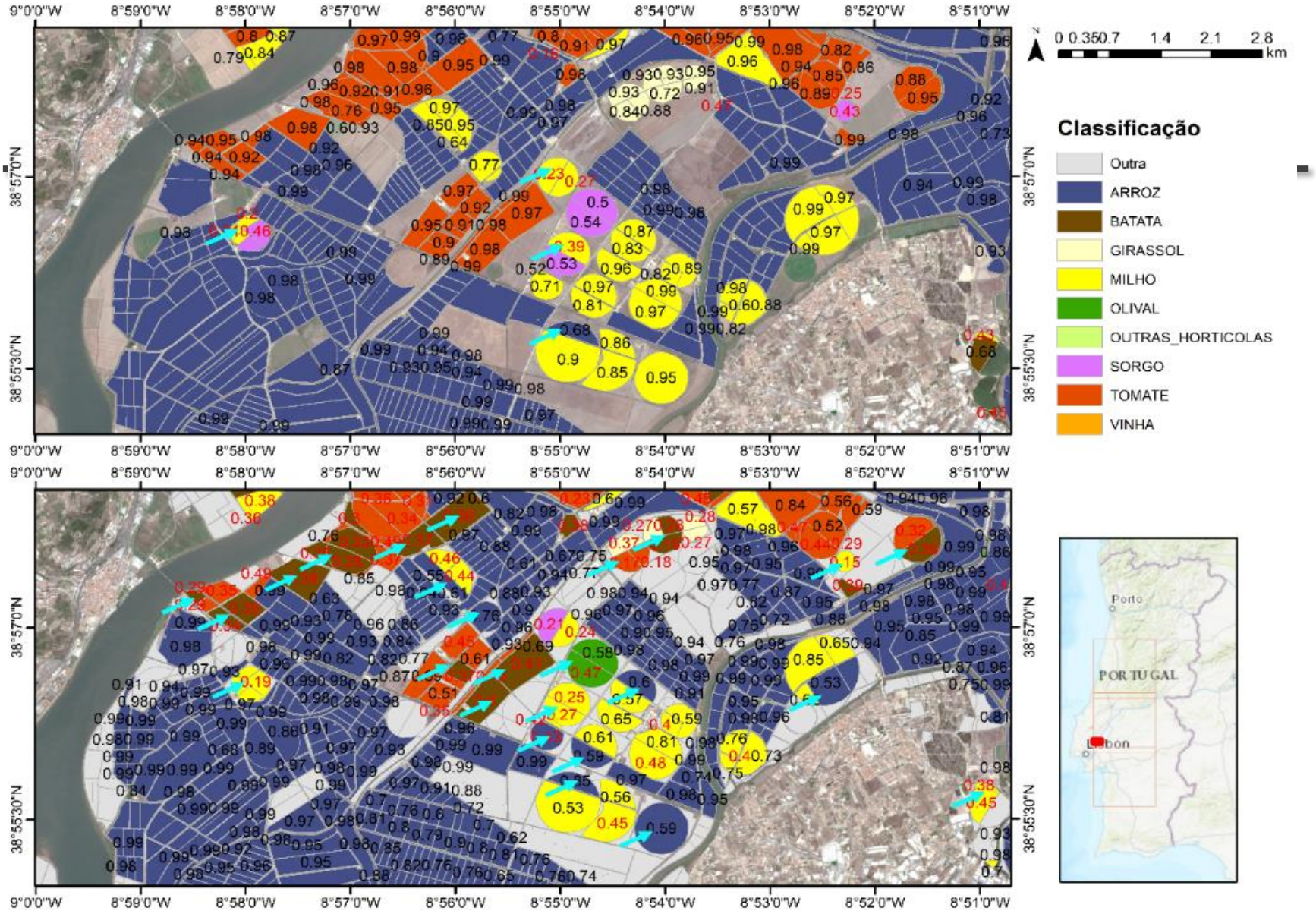

Mapa de confiança (2019 zona ND) para modelo sem TL (T02) e com TL (T06). Os valores iguais a 1 são omitidos; valores inferiores a 0.5 estão representados a vermelho

O sistema de monitorização SAMAS-IA

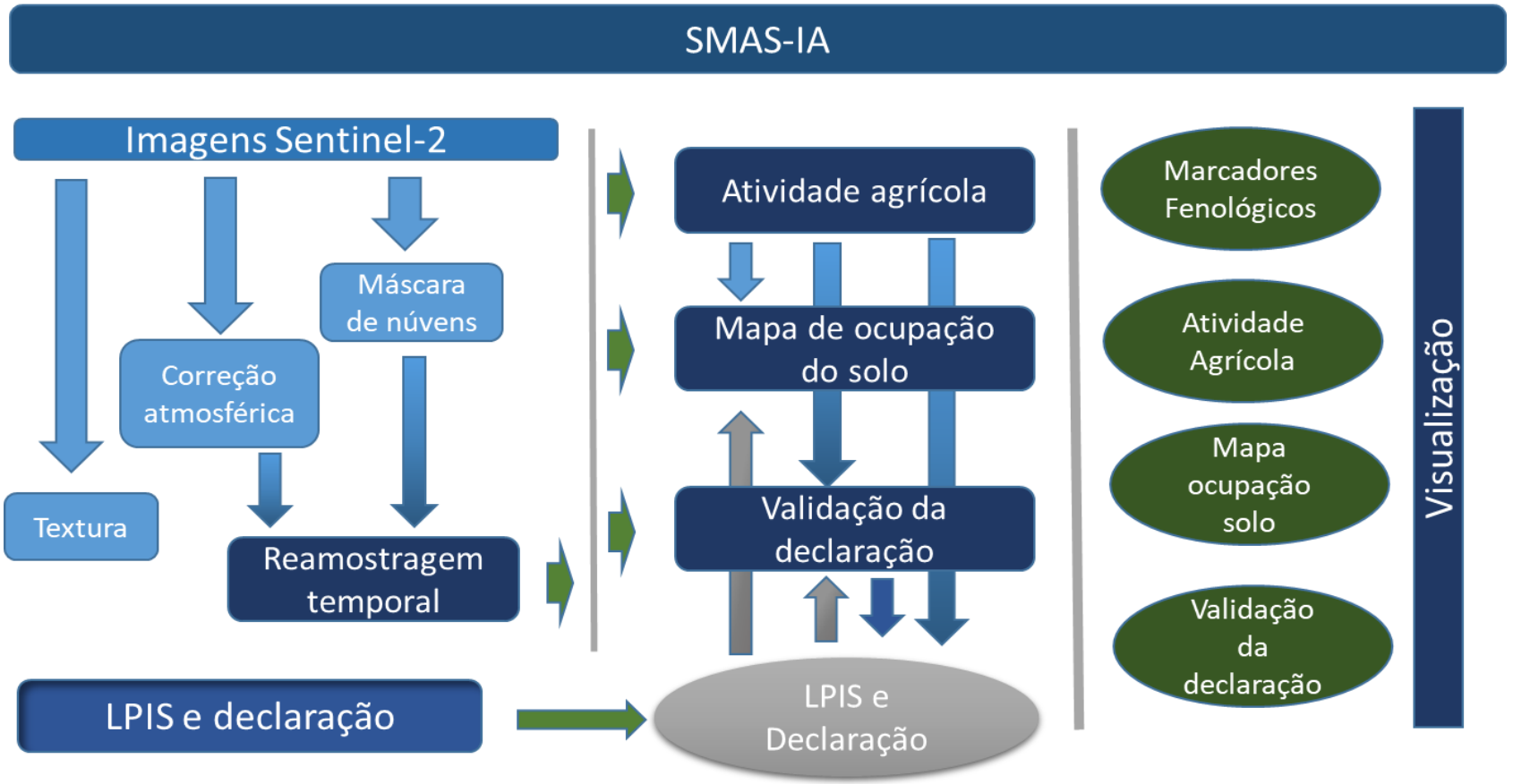

Validação da declaração

Mapa de ocupação do solo

LPIS e declaração

Atividade Agrícola

	Declarado cultura A				Declarado Vinha ou Olival			
Atividade agrícola	Sim	Não	Sim	Não	Não	Não	Não	Sim
Predito cultura A	Sim	Não	Não	Não	Sim	Não	Não	Não
Predito cultura B		Sim	Sim	Sim		Sim	Sim	Sim
Predito Cultura Temporária		Sim		Não			Sim	Sim
Predito Cultura Permanente			Sim	Sim		Sim		Não

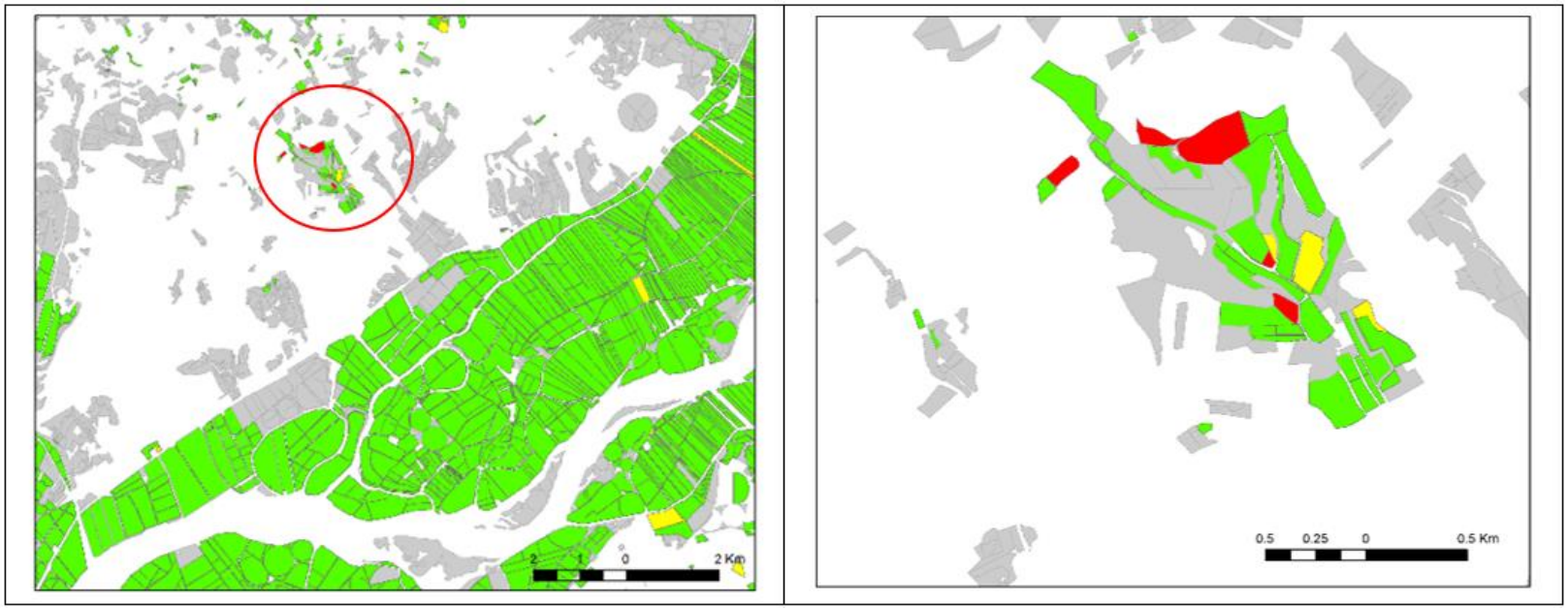

Monitorização do estado vegetativo do sobreiro com imagens multiespectrais do satélite Sentinel-2

João Catalão, Ana Navarro, João Calvão
IDL, Faculty of Sciences, University of Lisbon, Portugal;

GEOSUBER

Ciências ULisboa

remote sensing

MDPI

Article

Assessing the Use of Sentinel-2 Time Series Data for Monitoring Cork Oak Decline in Portugal

Ana Navarro *, Joao Catalao and Joao Calvao

Instituto Dom Luiz (IDL), Faculdade de Ciências, Universidade de Lisboa, 1749-016 Lisboa, Portugal; jcfernandes@fc.ul.pt (J.C.); jmrodrigues@fc.ul.pt (J.C.)

* Correspondence: acferreira@fc.ul.pt; Tel.: +351-217-500-030

Received: 27 September 2019; Accepted: 24 October 2019; Published: 28 October 2019

check for updates

Abstract: In Portugal, cork oak (*Quercus suber* L.) stands cover 737 Mha, being the most predominant species of the *montado* agroforestry system, contributing to the economic, social and environmental development of the country. Cork oak decline is a known problem since the late years of the 19th century that has recently worsened. The causes of oak decline seem to be a result of slow and cumulative processes, although the role of each environmental factor is not yet established. The availability of Sentinel-2 high spatial and temporal resolution dense time series enables monitoring of gradual processes. These processes can be monitored using spectral vegetation indices (VI) as their temporal dynamics are expected to be related with green biomass and photosynthetic efficiency. The Normalized Difference Vegetation Index (NDVI) is sensitive to structural canopy changes, however it tends to saturate at moderate-to-dense canopies. Modified VI have been proposed to incorporate the reflectance in the red-edge spectral region, which is highly sensitive to chlorophyll content while largely unaffected by structural properties. In this research, in situ data on the location and vitality status of cork oak trees are used to assess the correlation between chlorophyll indices (CI) and NDVI time series trends and cork oak vitality at the tree level. Preliminary results seem to be promising since differences between healthy and unhealthy (diseased/dead) trees were observed.

Keywords: *Quercus suber* L.; cork oak decline; Sentinel-2; time series; vegetation indices

Assessing the Use of Sentinel-2 Time Series Data for Monitoring Cork Oak Decline in Portugal

Ana Navarro *, Joao Catalao and Joao Calvao

Parcelas de referência

Parcela / Data	referência	2º voo	3º voo
Machoqueira	26 jun 2018	22 out 2018	25 jun 2019
C. Lezírias	12 jul 2018	23 out 2018	27 jun 2019
Freixo	10 jul 2018	24 out 2018	26 jun 2019
Azinhal	10 jul 2018	24 out 2018	24 jun 2019

Caraterísticas do VANT

> Sensefly eBee

> Câmara Sequoia com 4 bandas (Verde, Vermelho, Red-Edge e Infravermelho) + Visível (Azul, Verde e Vermelho)

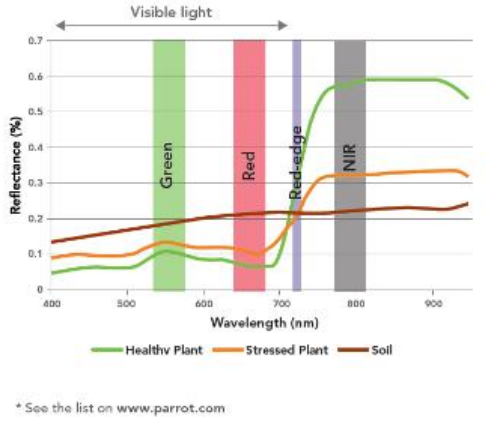

Ciências ULisboa

Assessing the Use of Sentinel-2 Time Series Data for Monitoring Cork Oak Decline in Portugal

Ana Navarro *, Joao Catalao and Joao Calvao

Companhia Lezirias

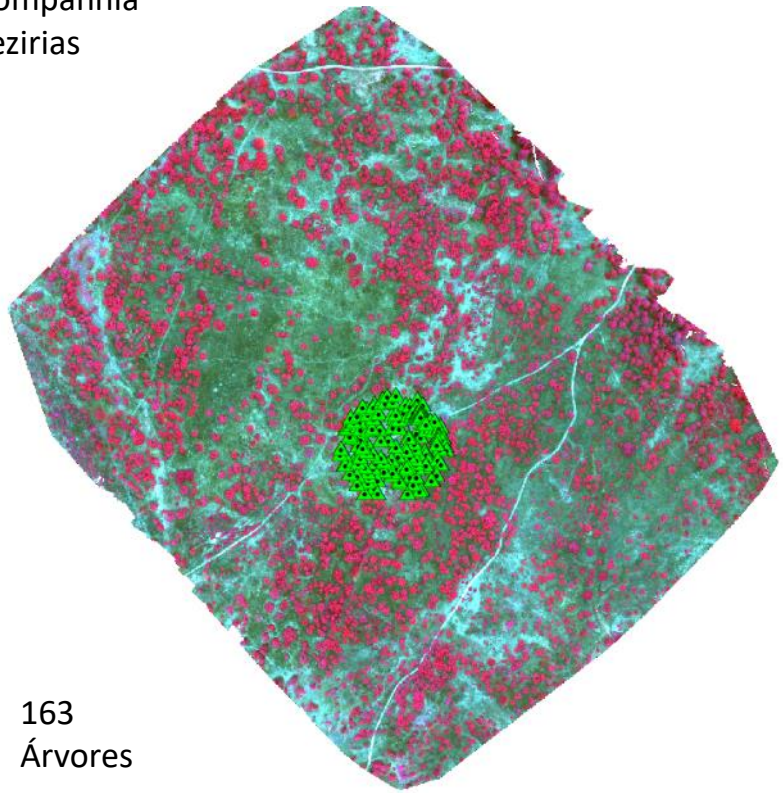

163 Árvores

Machoqueira

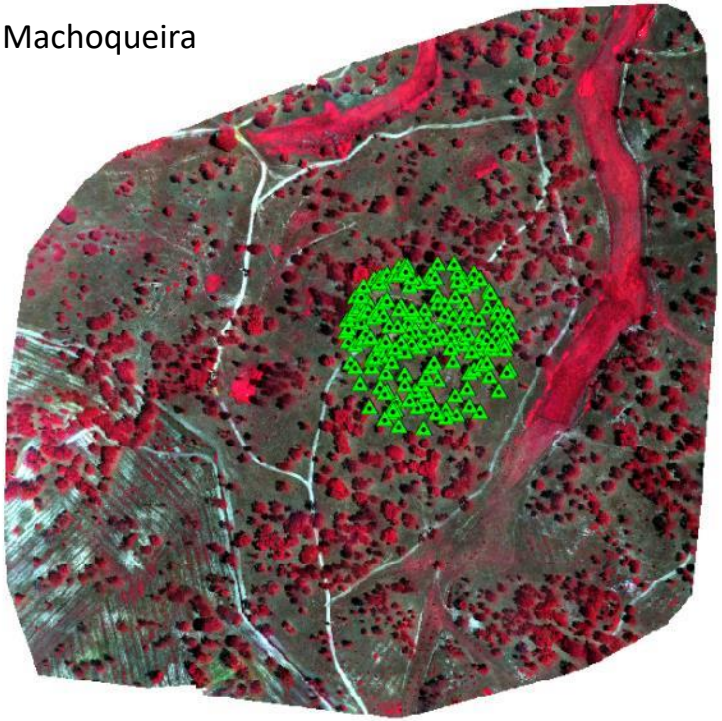

182 Árvores

C. Lezírias, UAV /S2 image

Identificação e georreferenciação de árvores no campo

Algoritmo para deteção de árvores

MSP

NDVI

Contorno
(Adapative binarization)

Euclidean Distance

Max Local

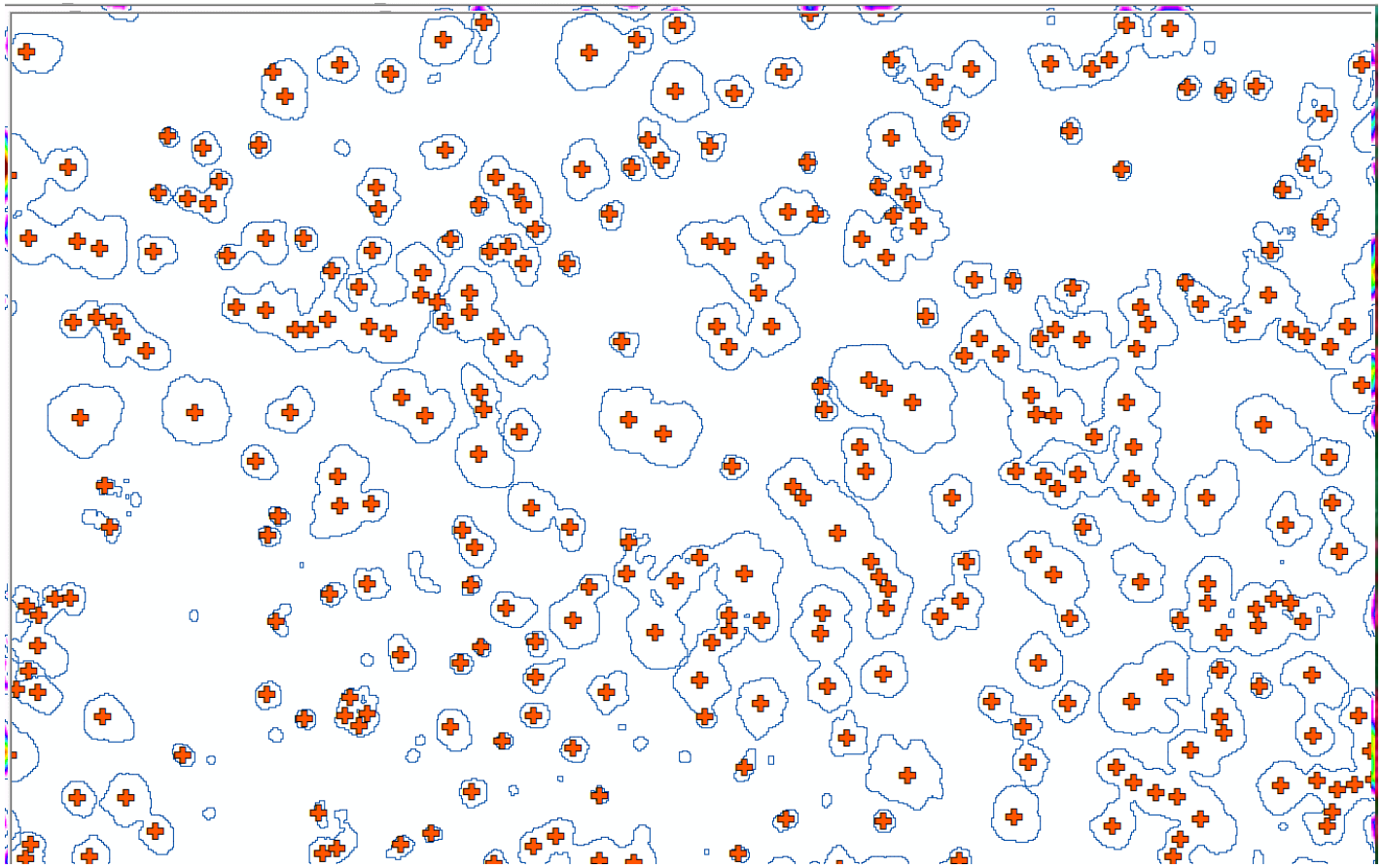

Algoritmo para deteção de árvores

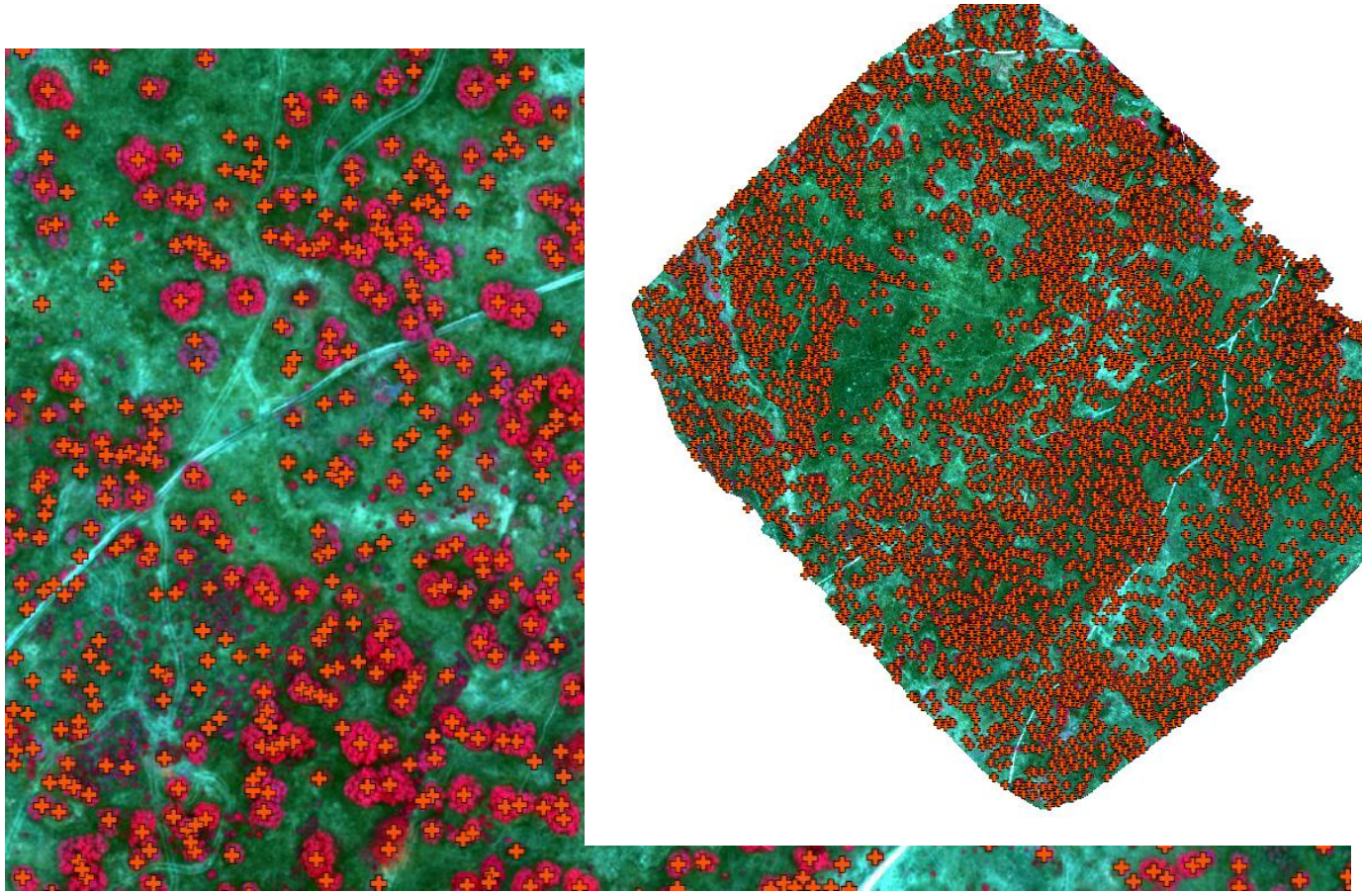

Ciências ULisboa

Assessing the Use of Sentinel-2 Time Series Data for Monitoring Cork Oak Decline in Portugal

Ana Navarro *, Joao Catalao and Joao Calvao

Análise Multitemporal

20160808	20170724	20180729
20160818	20170803	20180808
20160828	20170813	20180818
20160907	20170823	20180917
20160917	20170902	20180927
20160927	20170912	
20161007	20170922	
	20171002	
	20171012	
	20171022	

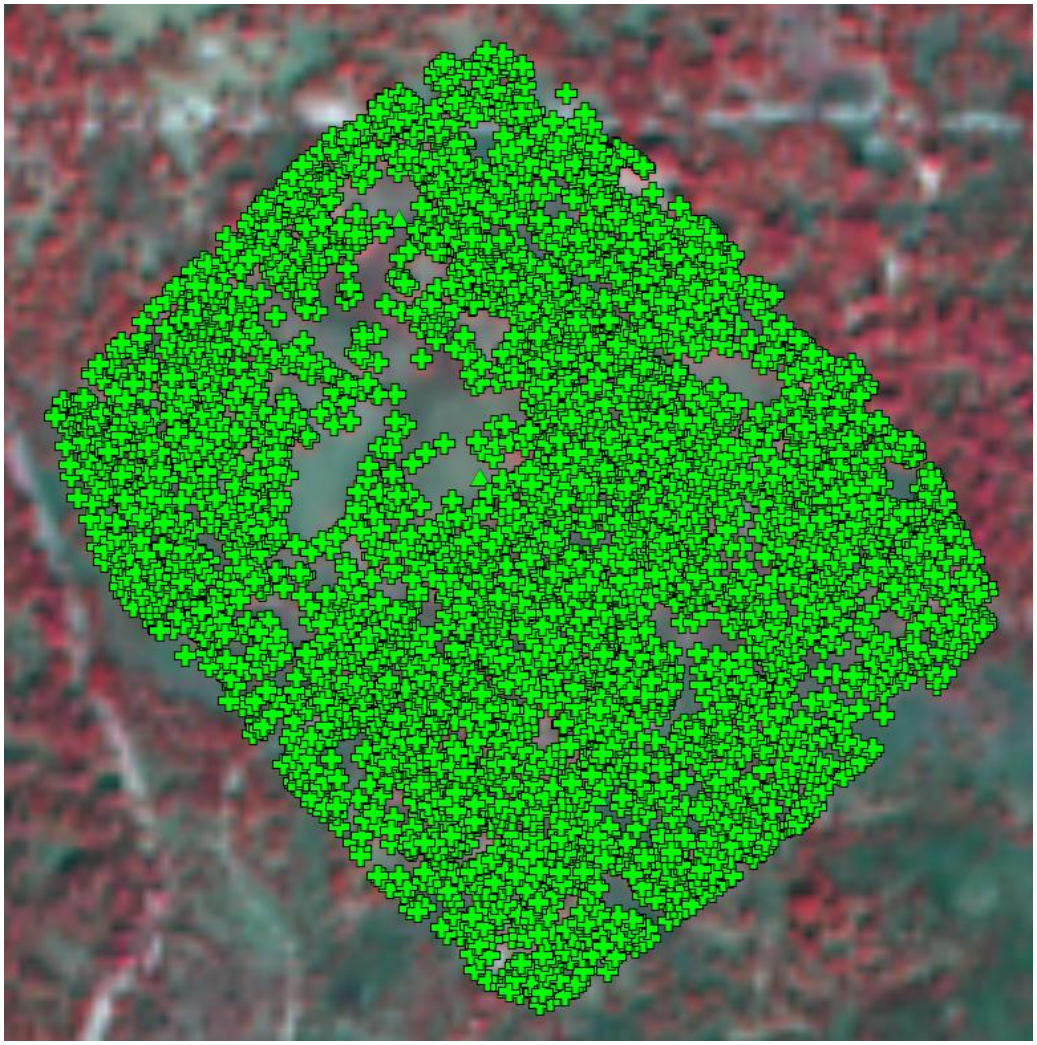

Ciências ULisboa

Assessing the Use of Sentinel-2 Time Series Data for Monitoring Cork Oak Decline in Portugal

Ana Navarro *, Joao Catalao and Joao Calvao

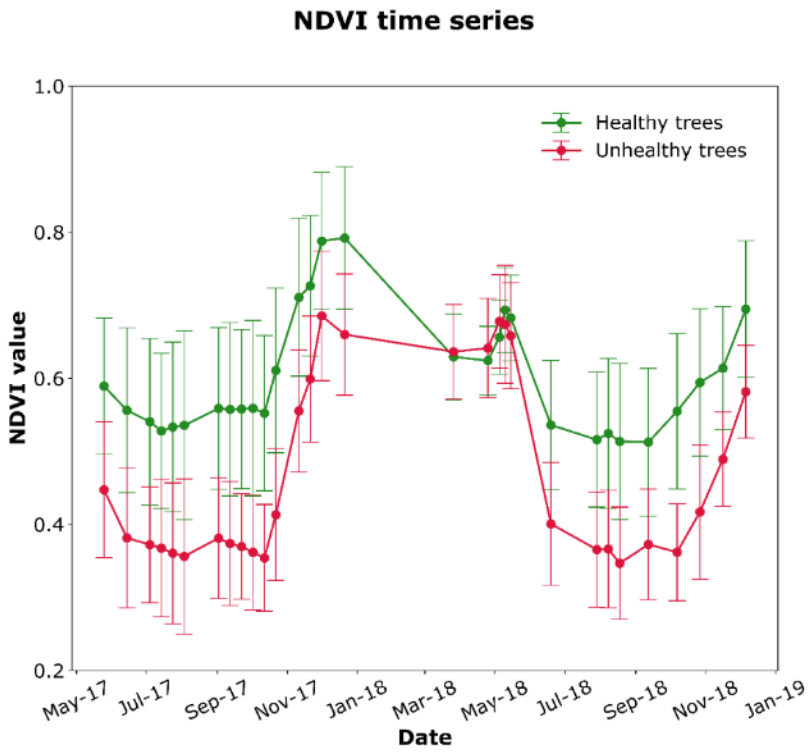

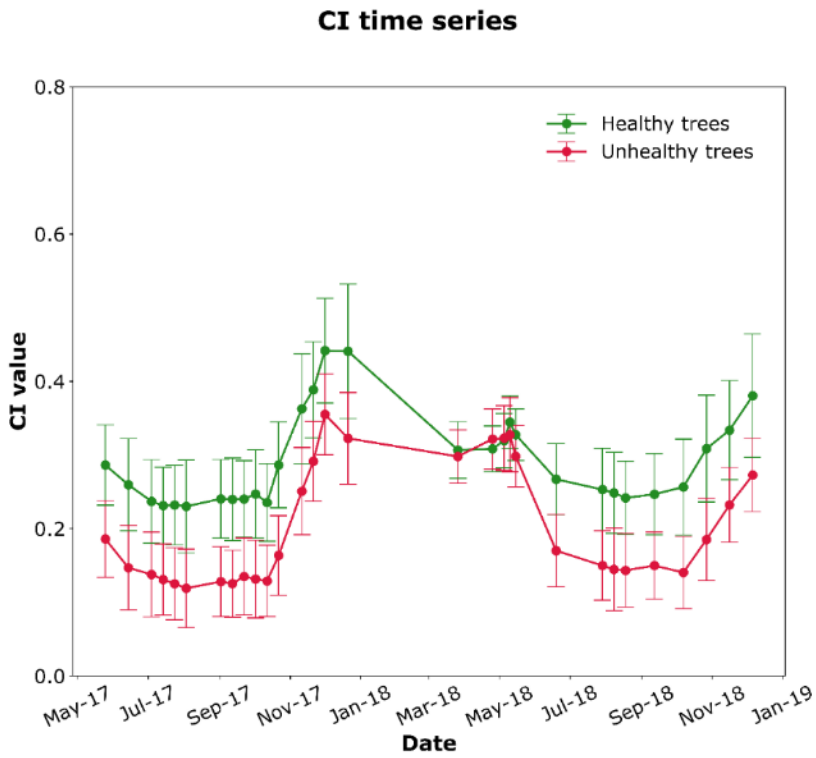

Série temporal dos indices NDVI e RedEdge

Ciências ULisboa

Assessing the Use of Sentinel-2 Time Series Data for Monitoring Cork Oak Decline in Portugal

Ana Navarro *, Joao Catalao and Joao Calvao

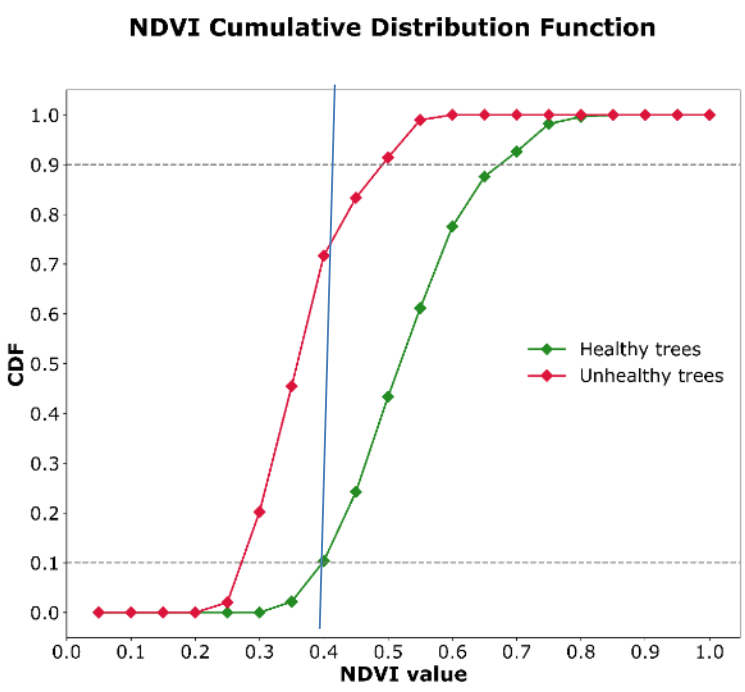

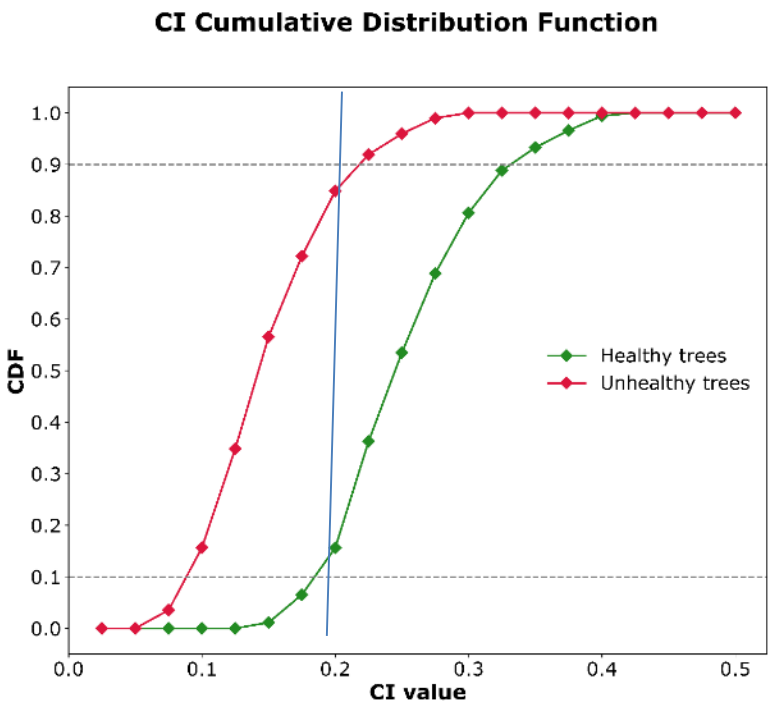

Função distribuição cumulativa do NDVI e RedEdge

Ciências ULisboa

Identificação das árvores com redução da atividade vegetativa

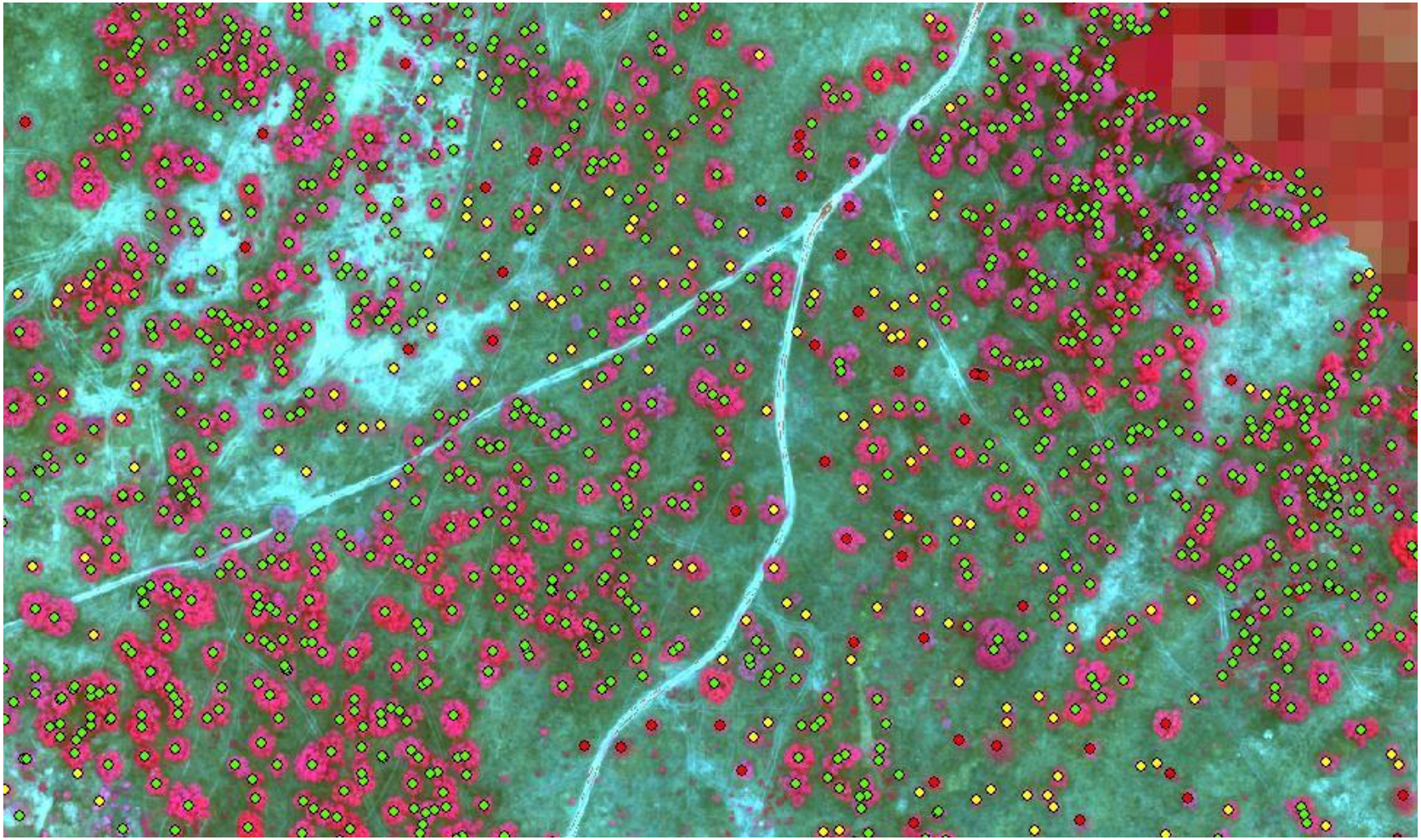

remote sensing

MDPI

Article

Mapping Cork Oak Mortality Using Multitemporal High-Resolution Satellite Imagery

João Catalão *, Ana Navarro and João Calvão

Instituto Dom Luiz, Faculdade de Ciências, Universidade de Lisboa, 1749-016 Lisboa, Portugal; acferreira@fc.ul.pt (A.N.); jmrodrigues@fc.ul.pt (J.C.)

* Correspondence: jcfernandes@fc.ul.pt; Tel.: +351-21-750-0833

Abstract: In the Mediterranean region, a significant decline in the vitality of vegetation has been observed in the last two decades, with a high forest mortality rate for several species. The increase in mortality has been attributed to water stress resulting from an increase in temperature and long periods of drought. To detect and quantify the impact of these events on tree mortality, an efficient and easy-to-use methodology for rapid damage assessment is required. Our study aims to assess the potential of high spatial resolution multispectral images from the Pleiades constellation to detect and map cork oak mortality in a pasture environment with multiple forest species. An approach based on change detection and the use of an unsupervised classifier is proposed to detect mortality at the cork oak level. The change in the values observed for three vegetation indices, NDVI, RGI, and GNDVI, between two epochs is used in an unsupervised classification algorithm to estimate the dead tree class. The classification results are accurate, with precision and recall values higher than 90%. Detailed cork oak mortality mapping is of significant use in comprehending ecosystem change as a result of tree mortality and for the implementation of mitigation mechanisms for the ongoing desertification process.

Mapping Cork Oak Mortality Using Multitemporal High-Resolution Satellite Imagery

João Catalão *, Ana Navarro and João Calvão

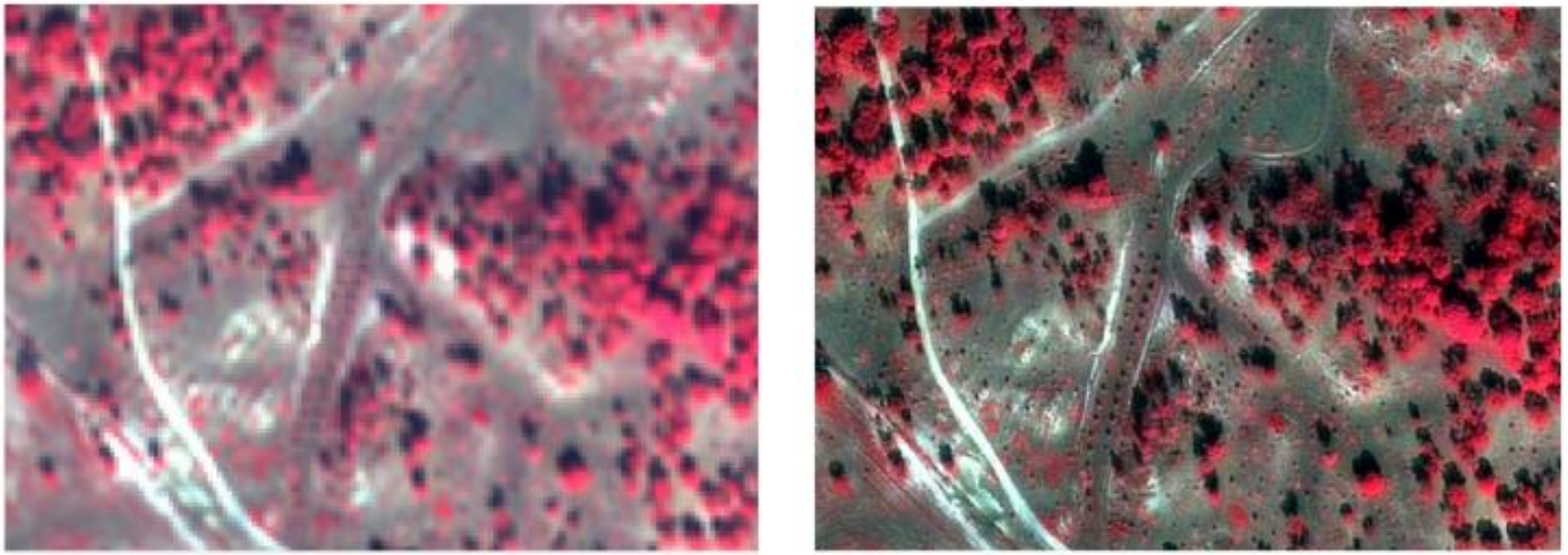

Figure 2. False-color composite of the multispectral image acquired in 2018 (**left**) and the corresponding pan-sharpened image (**right**).

Ciências ULisboa

Mapping Cork Oak Mortality Using Multitemporal High-Resolution Satellite Imagery

João Catalão *, Ana Navarro and João Calvão

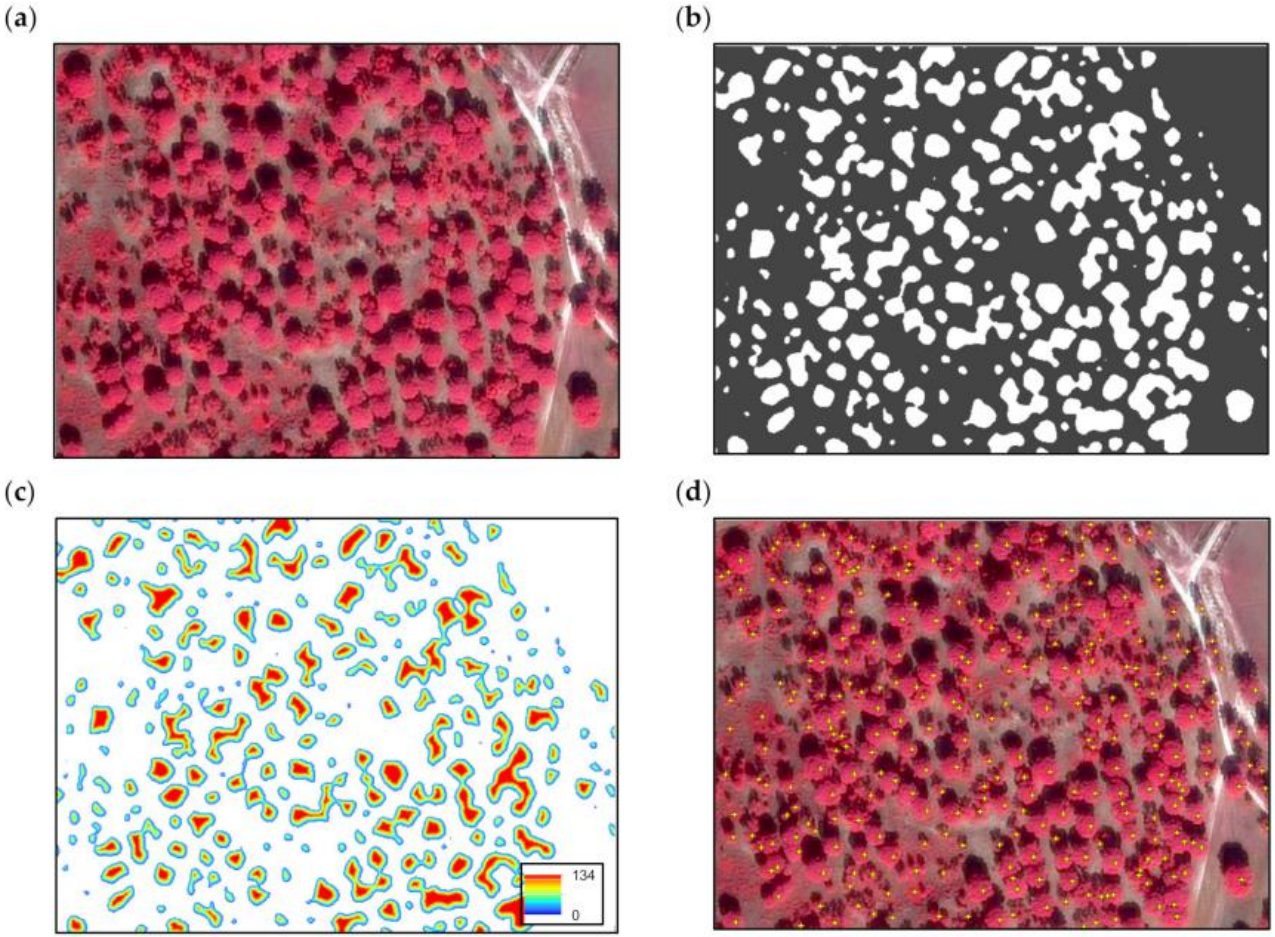

Figure 3. (**a**) False-color image (NIR, R, G); (**b**) Adaptative binarization; (**c**) Euclidean distance map; (**d**) Individual tree location obtained using the developed algorithm (yellow cross).

Mapping Cork Oak Mortality Using Multitemporal High-Resolution Satellite Imagery

Ciências ULisboa

João Catalão *, Ana Navarro and João Calvão

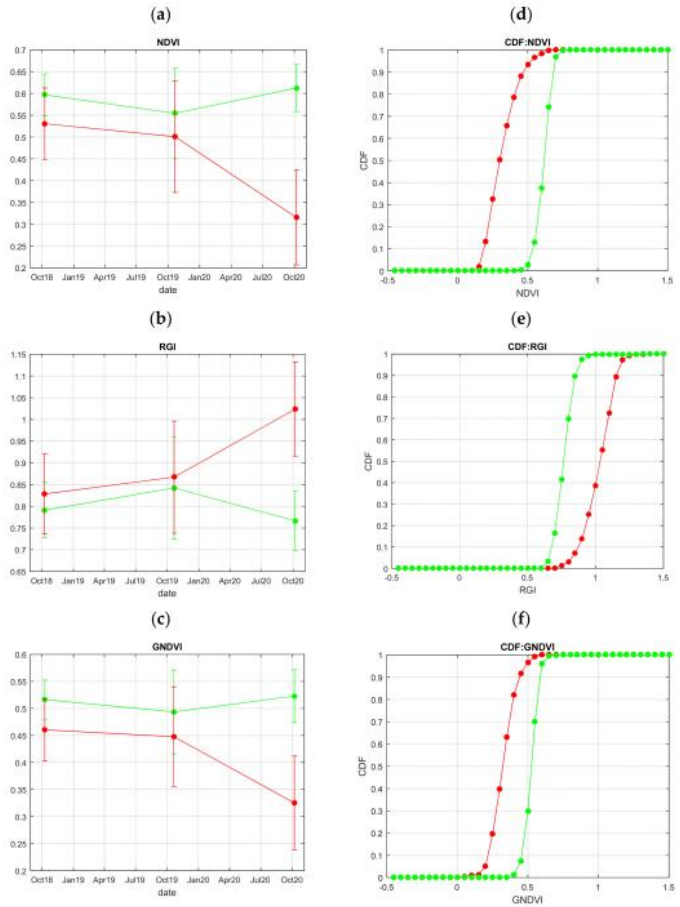

Figure 4. Healthy (green) and dead (red) trees' temporal variability is computed based on the NDVI (**a**), RGI (**b**), and GNDVI (**c**) indices. Cumulative distribution function (CDF) applied to NDVI (**d**), RGI (**e**), and GNDVI (**f**). Green lines show the cumulative probability of healthy trees while red lines

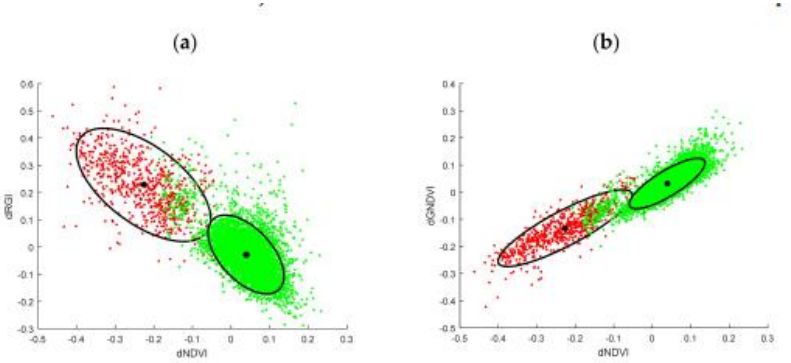

Figure 5. Distribution of dead trees (red) and healthy trees (green) in the indices feature space: (**a**) ΔNDVI versus ΔRGI and (**b**) ΔNDVI versus ΔGNDVI. The 90% confidence ellipse for each of the trees' classes is drawn in black.

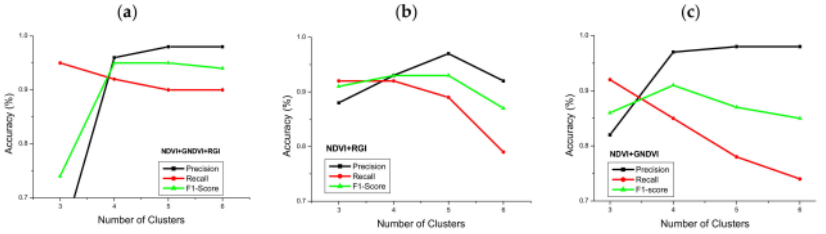

Figure 6. Classification accuracy as a function of the number of clusters used in the k-means classification for the three-band combinations: (**a**) ΔNDVI, ΔRGI, ΔGNDVI, (**b**) ΔNDVI, ΔRGI and (**c**) ΔNDVI, ΔGNDVI.

Ciências ULisboa

Mapping Cork Oak Mortality Using Multitemporal High-Resolution Satellite Imagery

João Catalão *, Ana Navarro and João Calvão

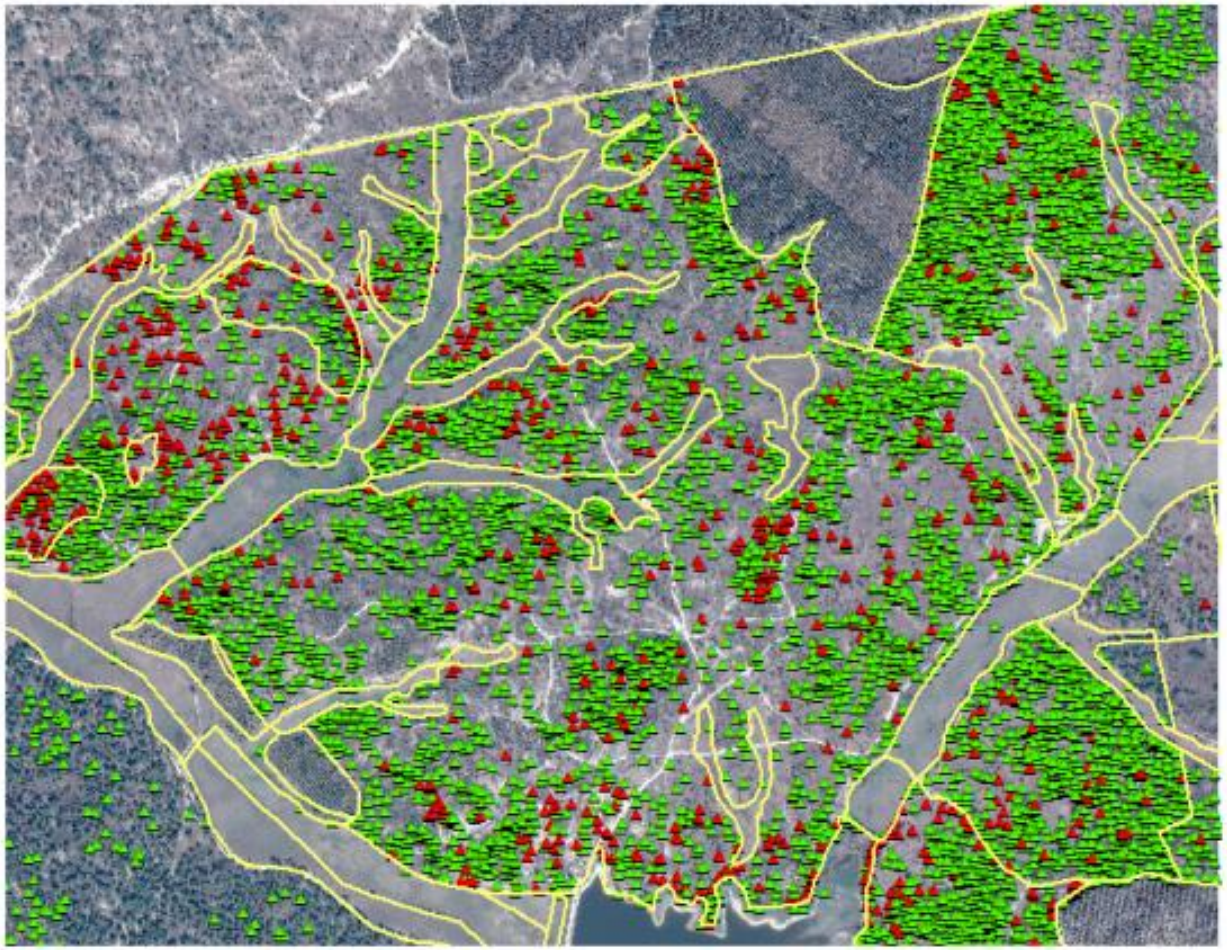

Figure 8. Results of the multitemporal tree classification for the study area. Red triangles represent dead trees and green triangles represent healthy trees, superimposed on the Pleiades image.

Multitemporal Backscattering Logistic Analysis for Intertidal Bathymetry

J. Catalão, *Member, IEEE*, and G. Nico, *Senior Member, IEEE*

***Abstract*— A new methodology for the mapping of intertidal terrain morphology is presented. It is based on the use of synthetic aperture radar (SAR) images and the temporal correlation between the SAR backscatter intensity and the water level on the intertidal zone. The proposed methodology does not require manual editing, providing a set of geolocated pixels that can be used to generate a digital elevation model of the intertidal zone. The methodology is validated using TerraSAR-X SAR images acquired over Tagus estuary. This methodology can be useful for the regular updating of intertidal bathymetric models useful for both flood hazard mitigation and morphodynamics modeling.**

***Index Terms*— Digital elevation model (DEM), intertidal bathymetry, morphodynamic modeling, synthetic aperture radar (SAR).**

I. Introduction

THE coastal environment is a complex system exposed to external forces acting at different spatial and tempo-

The height of the waterline is predicted by a hydrodynamic tide model. The intertidal bottom topography model is generated by stacking several waterlines extracted in different tide conditions. The method can be used with both synthetic aperture radar (SAR) and optical spaceborne systems [5], [6]. The main advantage of SAR systems over optical ones is their capability of working in all weather and solar illumination conditions. In the absence of wind or rain, the water surface is generally smooth and can be assumed as a specular reflector with small backscatter intensity. On the contrary, land surface is generally irregular and rough and it behaves as a diffuse scattering surface with moderate to high backscatter intensity. Thus, in SAR images, water appears with a homogeneous moderate intensity, whereas land surface corresponds to higher intensities, depending on the surface orientation. Therefore, the waterline extraction may be considered a threshold prob-

Ciências ULisboa

Multitemporal Backscattering Logistic Analysis for Intertidal Bathymetry

J. Catalão, *Member, IEEE*, and G. Nico, *Senior Member, IEEE*

Waterline Method

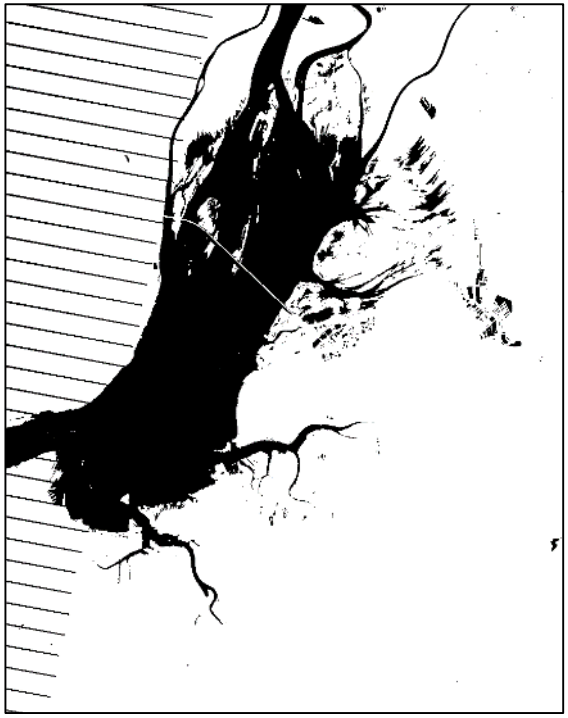

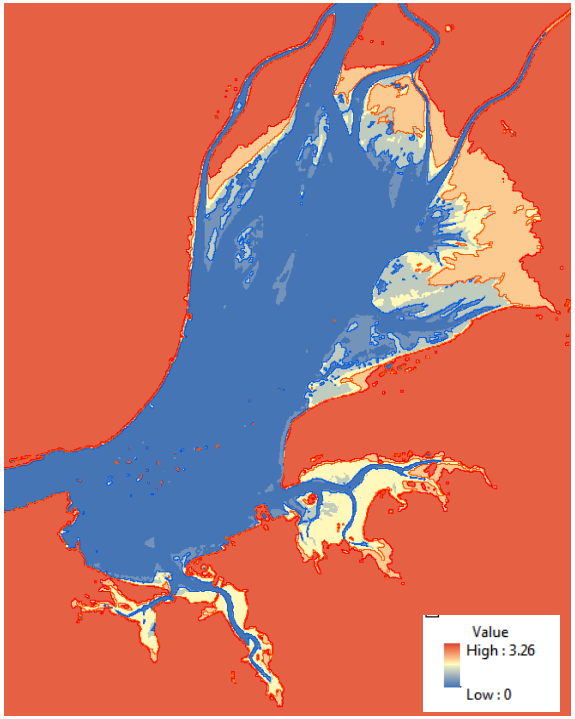

Water level = 0.69 m
Date: 31 Aug. 2007

Ciências ULisboa

Multitemporal Backscattering Logistic Analysis for Intertidal Bathymetry

J. Catalão, *Member, IEEE*, and G. Nico, *Senior Member, IEEE*

Multitemporal Intensity Logistic Analysis (MILA)

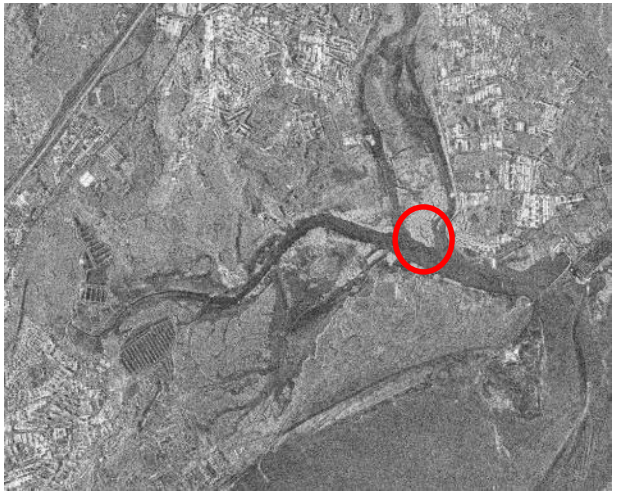

Low tide

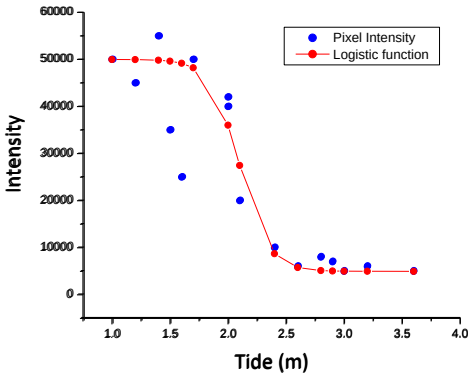

High tide

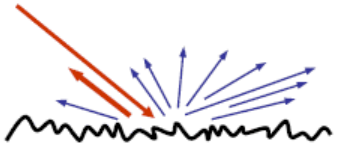

Diffuse to Specular scattering

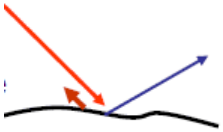

Ciências ULisboa

Multitemporal Backscattering Logistic Analysis for Intertidal Bathymetry

J. Catalão, *Member, IEEE*, and G. Nico, *Senior Member, IEEE*

Logistic analysis

The logistic function relates the height of the resolution cell (h) with the pixel intensity (J_i). The function is defined by the parameters (a, k, h) and is given by:

$$J_i = \frac{k}{1 + e^{-a(h_i - h)}} \qquad i = 1, .., M$$

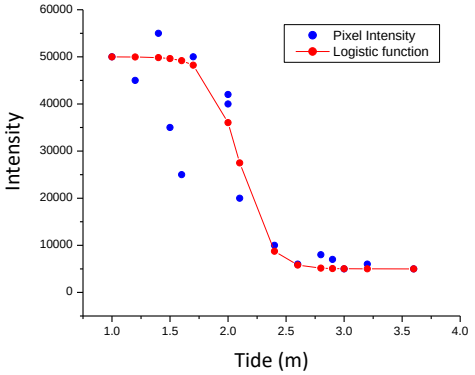

In which **k** is the maximum intensity, **a** is the steepness of the logistic function (a= -8, if negative the function decrease), h is the height of the resolution cell and h_i is the tide height for image i.

$$\min\left\{\sum_{i=1}^{M} h_i - h + \frac{1}{a}\ln\left(\frac{J_i}{k - J_i}\right)\right\}^2$$

h and k are the parameters to be estimated

We have to search on the solution space for the values (h, k) that minimize the expression.

Ciências ULisboa

Multitemporal Backscattering Logistic Analysis for Intertidal Bathymetry

J. Catalão, *Member, IEEE*, and G. Nico, *Senior Member, IEEE*

Intertidal elevation model

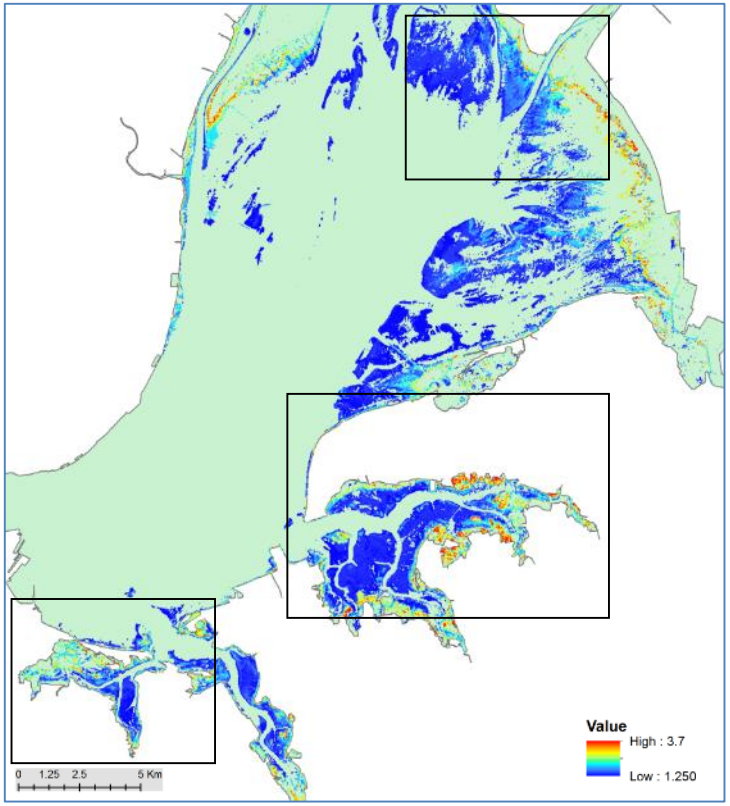

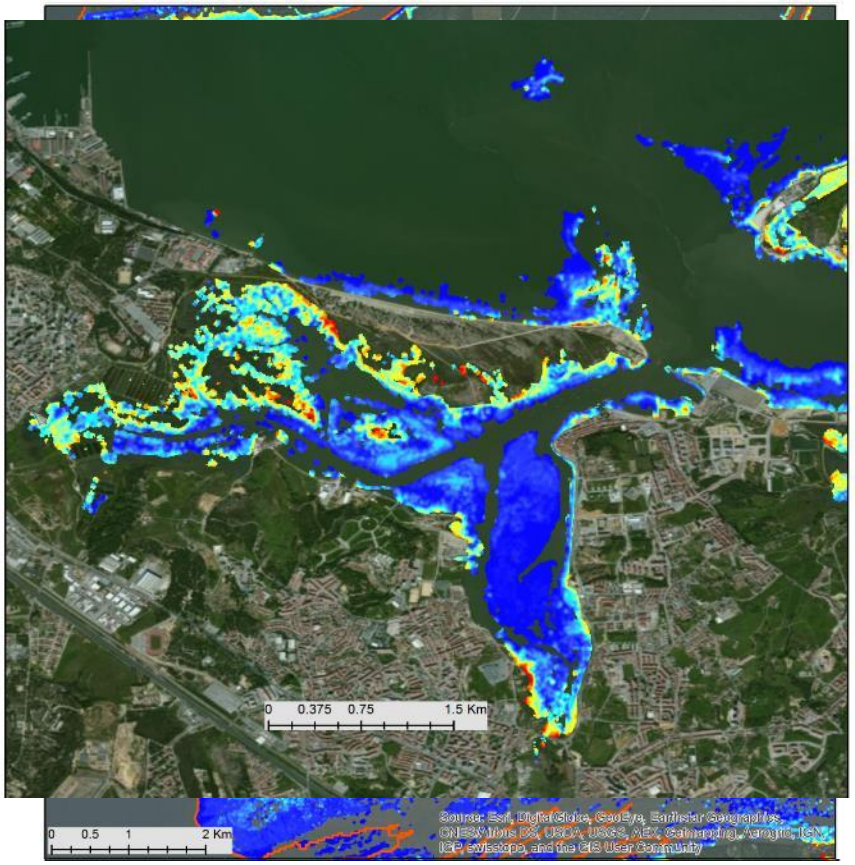

Intertidal Bathymetry Extraction with Multispectral Images: A Logistic Regression Approach

Isabel Bué [1,2], João Catalão [2,*] and Álvaro Semedo [2,3]

Ciências ULisboa

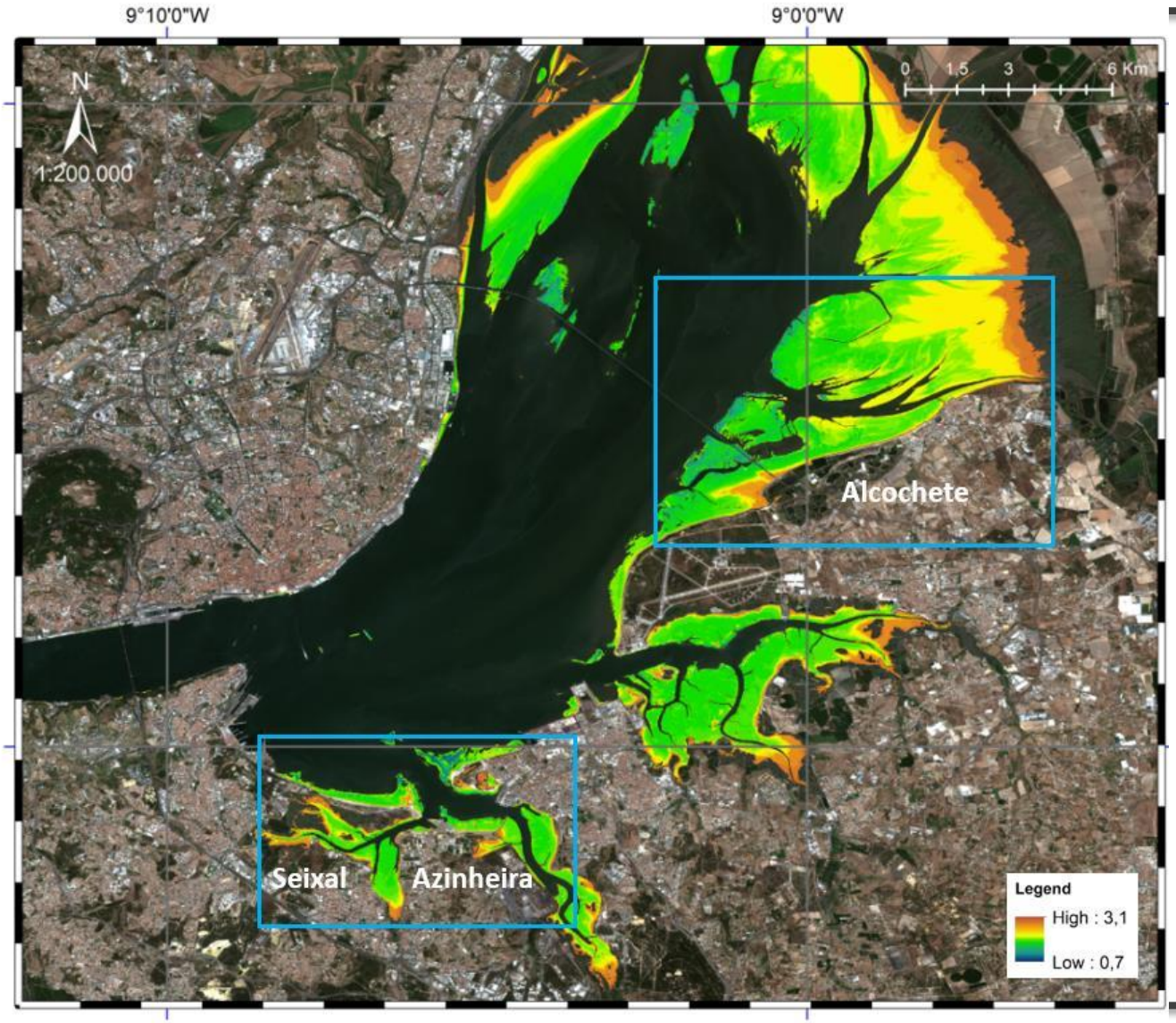

Sentinel-2 - Tejo

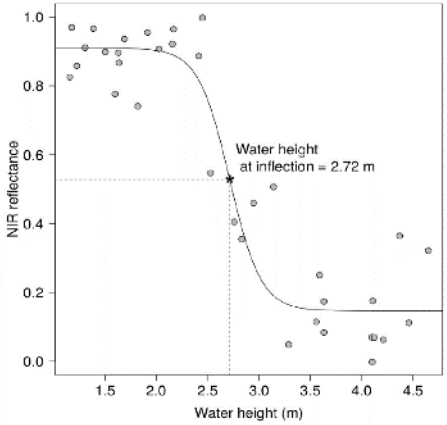

Bué et al., 2020

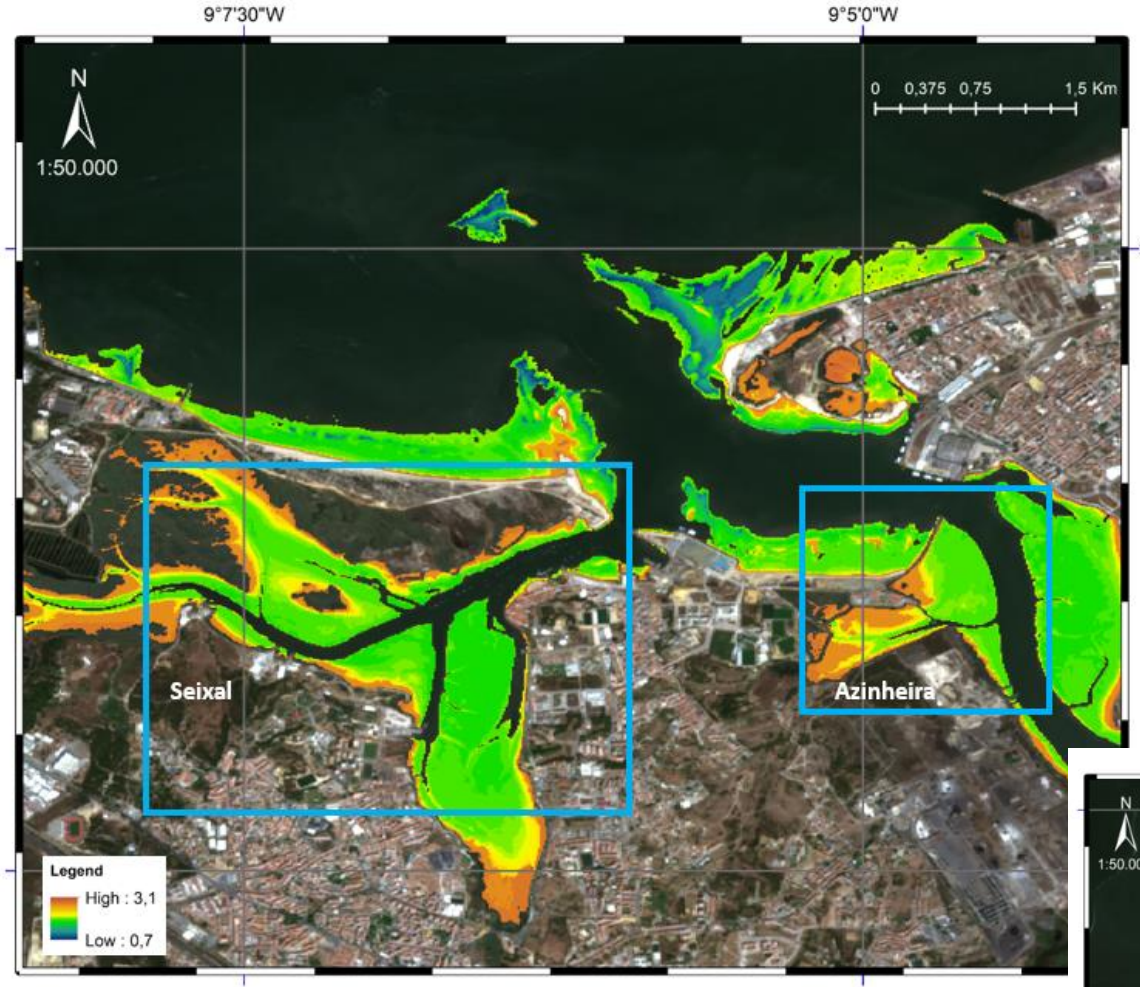

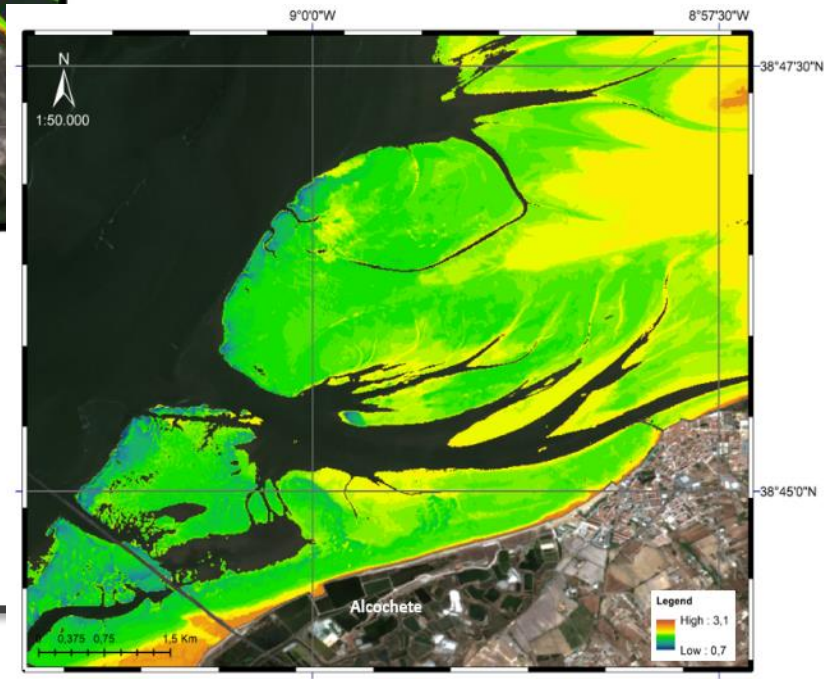

Intertidal Bathymetry Extraction with Multispectral Images: A Logistic Regression Approach

Isabel Bué [1,2], João Catalão [2,*] and Álvaro Semedo [2,3]

Ciências ULisboa

Using Sentinel-2 Images to Estimate Topography, Tidal-Stage Lags and Exposure Periods over Large Intertidal Areas

José P. Granadeiro [1,*,†], João Belo [1,†], Mohamed Henriques [1], João Catalão [2] and Teresa Catry [1]

Sentinel-2 - Bijagós

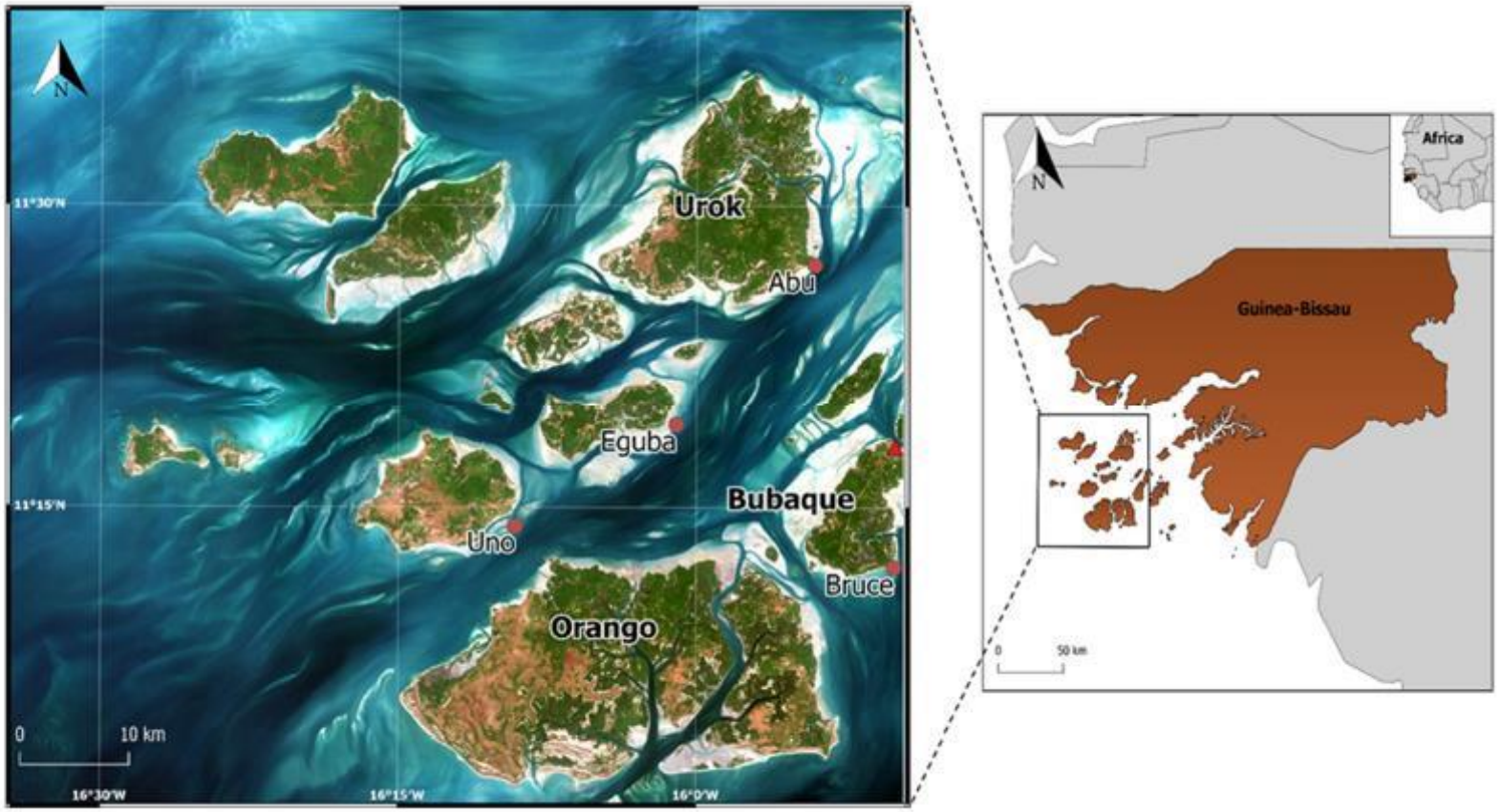

Granadeiro et al., 2022

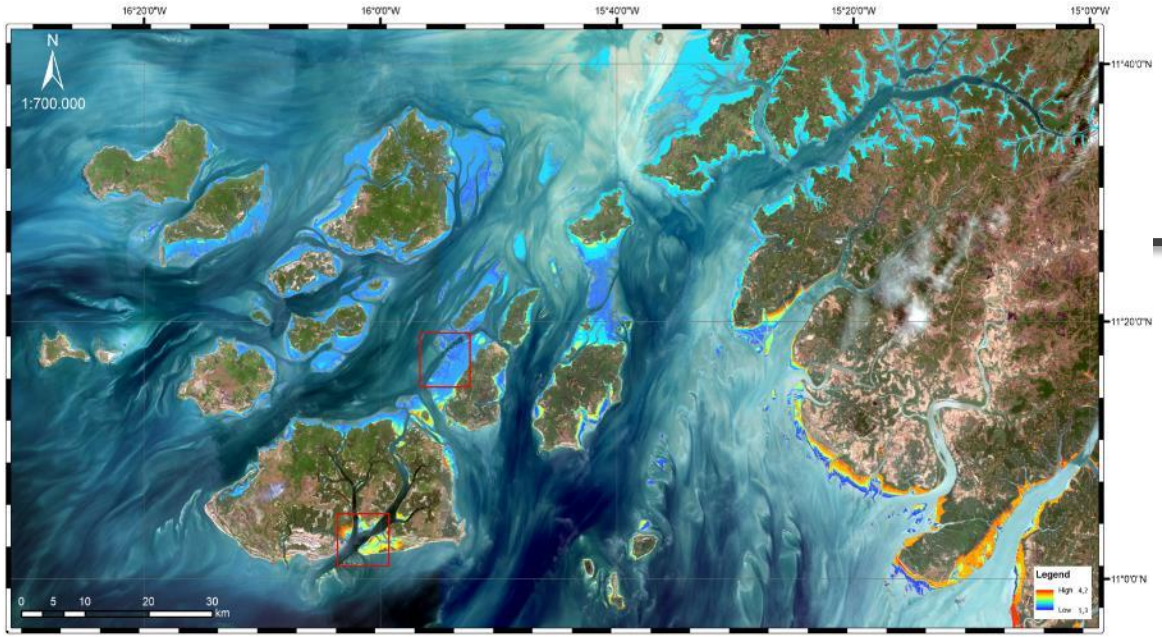

Using Sentinel-2 Images to Estimate Topography, Tidal-Stage Lags and Exposure Periods over Large Intertidal Areas

José P. Granadeiro [1,*,†], João Belo [1,†], Mohamed Henriques [1], João Catalão [2] and Teresa Catry [1]

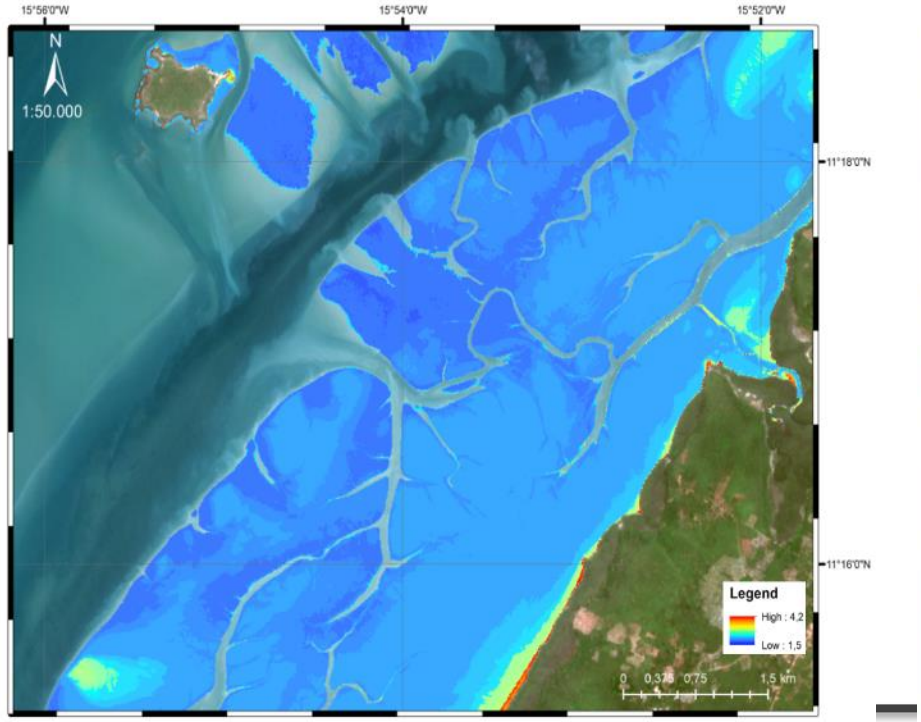

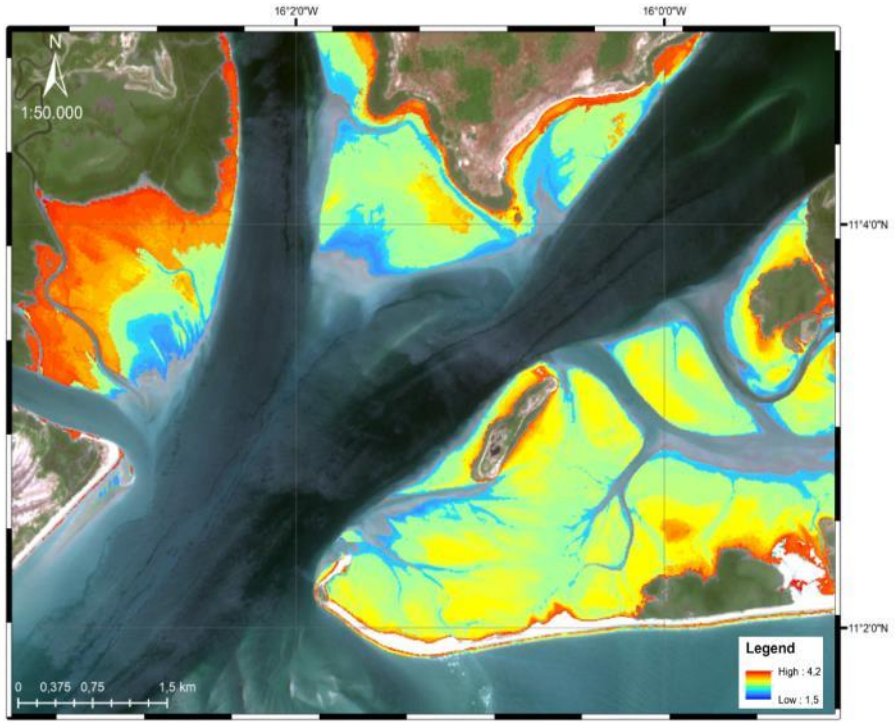

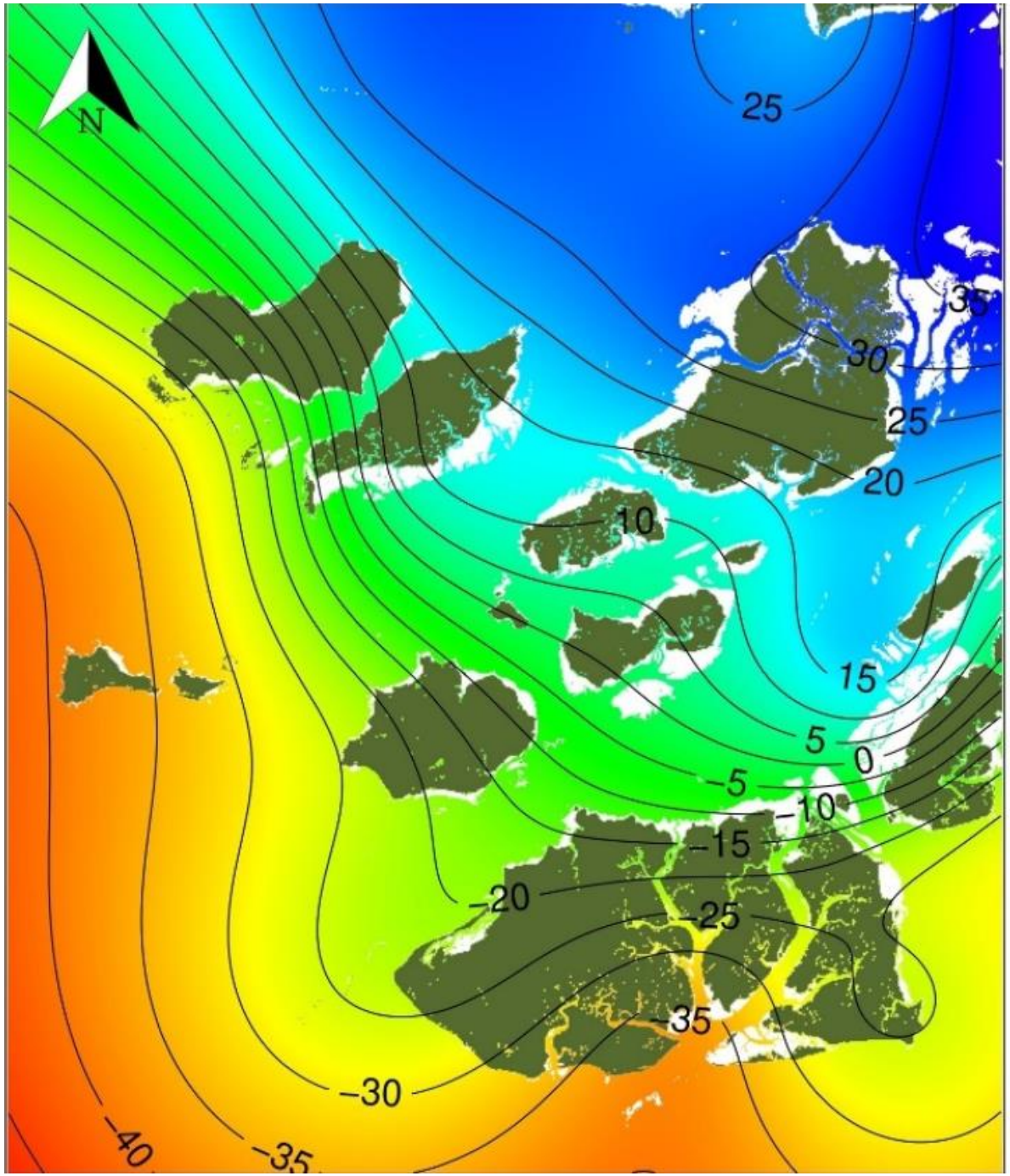

Using Sentinel-2 Images to Estimate Topography, Tidal-Stage Lags and Exposure Periods over Large Intertidal Areas

José P. Granadeiro [1,*,†], João Belo [1,†], Mohamed Henriques [1], João Catalão [2] and Teresa Catry [1]

Figure 9. Cotidal lines, showing the time-lag (in min) from the reference point in Bubaque, estimated using data from 50,000 random intertidal pixels as a function of longitude and latitude, using a generalized additive model (GAM) with thin-plate regression splines

remote sensing

MDPI

Article

Detecting Deforestation Using Logistic Analysis and Sentinel-1 Multitemporal Backscatter Data

Adrian Dascălu [1], João Catalão [2,*] and Ana Navarro [2]

[1] Faculty of Hydrotechnics, Geodesy and Environmental Engineering, Technical University "Gheorghe Asachi", 70050 Iasi, Romania
[2] Universidade de Lisboa, Faculdade de Ciências, Instituto Dom Luiz, 1749-016 Lisboa, Portugal
* Correspondence: jcfernandes@fc.ul.pt

Abstract: This paper presents a new approach for detecting deforestation using Sentinel-1 C-band backscattering data. It is based on the temporal analysis of the backscatter intensity and its correlation with the scattering behavior of deforested plots. The backscatter intensity temporal variability is modeled with a logistic function, whose lower and upper boundaries are, respectively, set based on the representative backscatter values for forest and deforested plots. The approach also enables the identification of the date of each deforestation event, corresponding to the inflection point of the logistic curve that best fits the backscatter intensity time series. The methodology was applied to two forest biomes, a tropical forest at Iguazu National Park in Argentina and a temperate forest in the Brăila region in Romania. The optimal flattening parameter was 0.12 for both sites, with an F1-score of 0.93 and 0.71 for the tropical and temperate forests, respectively. The temporal accuracy shows a bias on the estimated date, with a slight delay of 2 months. The results reveal that the Sentinel

Detecting Deforestation Using Logistic Analysis and Sentinel-1 Multitemporal Backscatter Data

Adrian Dascălu [1], João Catalão [2,*] and Ana Navarro [2]

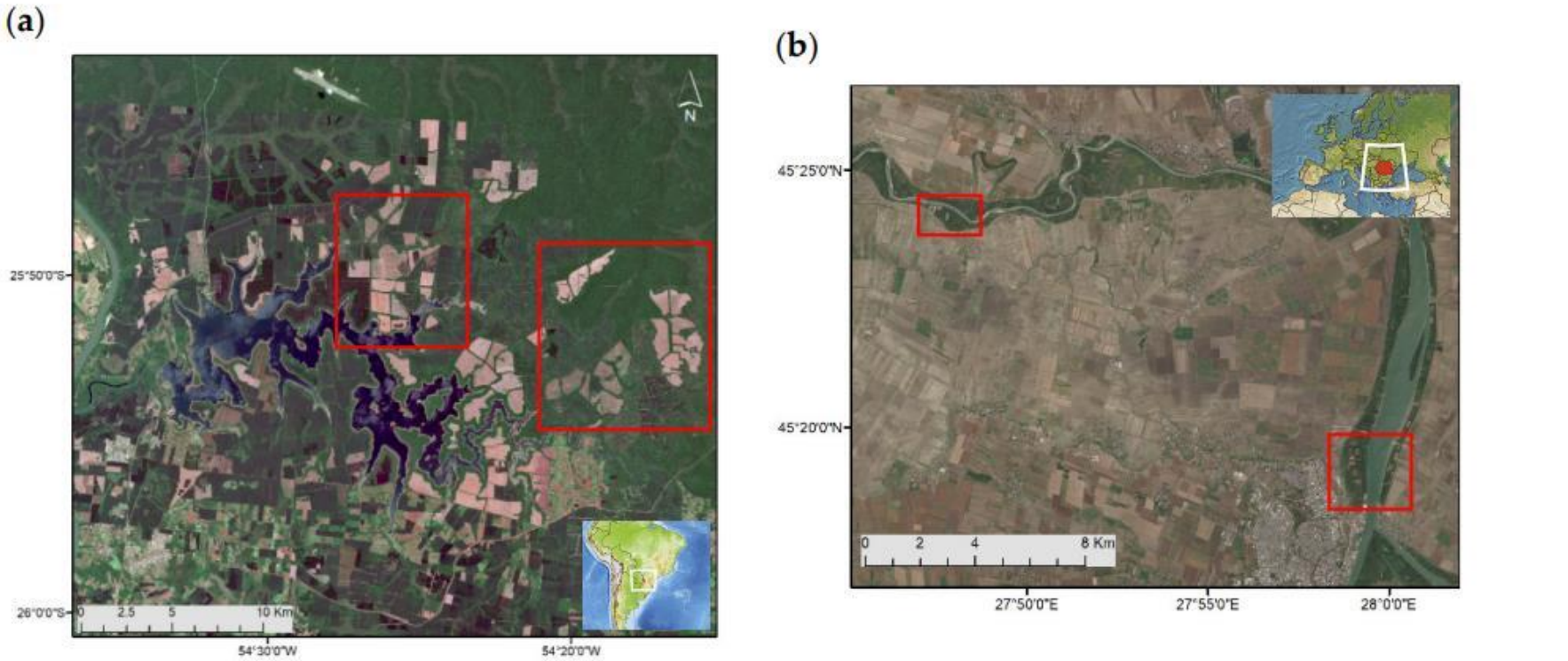

Figure 1. Sentinel-2 images for both test areas: (**a**) Iguazu National Park (Argentina, South America), December 2021, and (**b**) Brăila (Romania, Europe), September 2020. Red rectangles correspond to insets of the test areas adopted for results presentation and discussion.

Detecting Deforestation Using Logistic Analysis and Sentinel-1 Multitemporal Backscatter Data

Adrian Dascălu [1], João Catalão [2,*] and Ana Navarro [2]

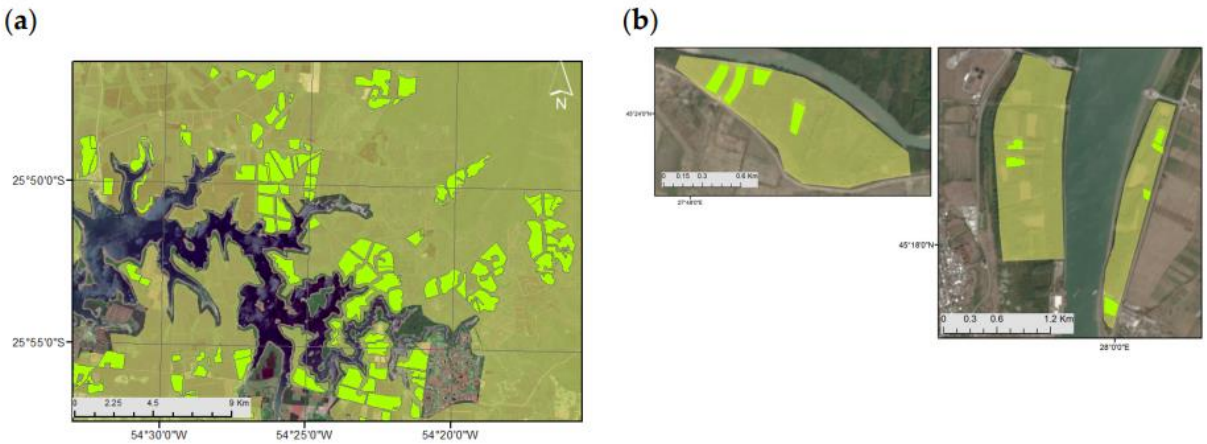

Figure 2. Deforestation reference data (green polygons) and forest mask (light yellow mask) overlaid on Sentinel-2 images: (**a**) Iguazu National Park and (**b**) Brăila.

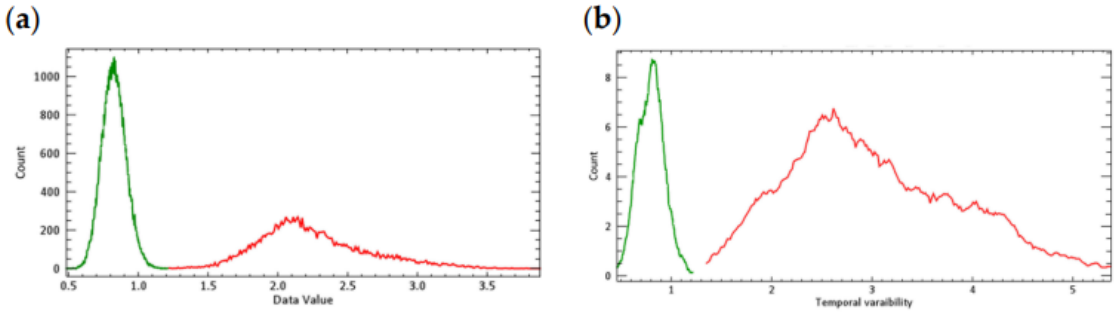

Figure 3. Frequency distribution of temporal standard deviation of stable forest (green line) and deforested areas (red line) for (**a**) Iguazu and (**b**) Brăila.

Detecting Deforestation Using Logistic Analysis and Sentinel-1 Multitemporal Backscatter Data

Adrian Dascălu [1], João Catalão [2,*] and Ana Navarro [2]

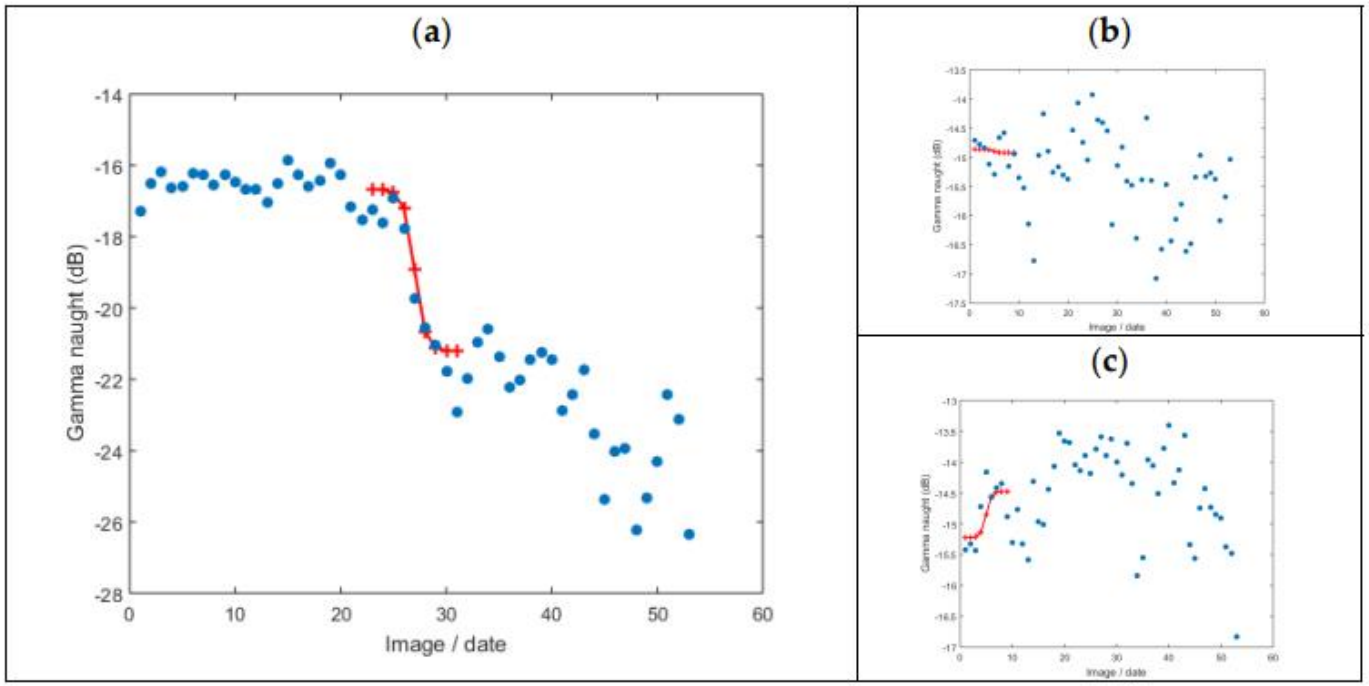

Figure 4. (**a**) Backscatter intensity (gamma-naught) as a function of the image /date (blue dots) overlaid with the fitted logistic function (red line); (**b**) flat logistic curve and (**c**) inverted logistic curve.

Detecting Deforestation Using Logistic Analysis and Sentinel-1 Multitemporal Backscatter Data

Adrian Dascălu [1], João Catalão [2,*] and Ana Navarro [2]

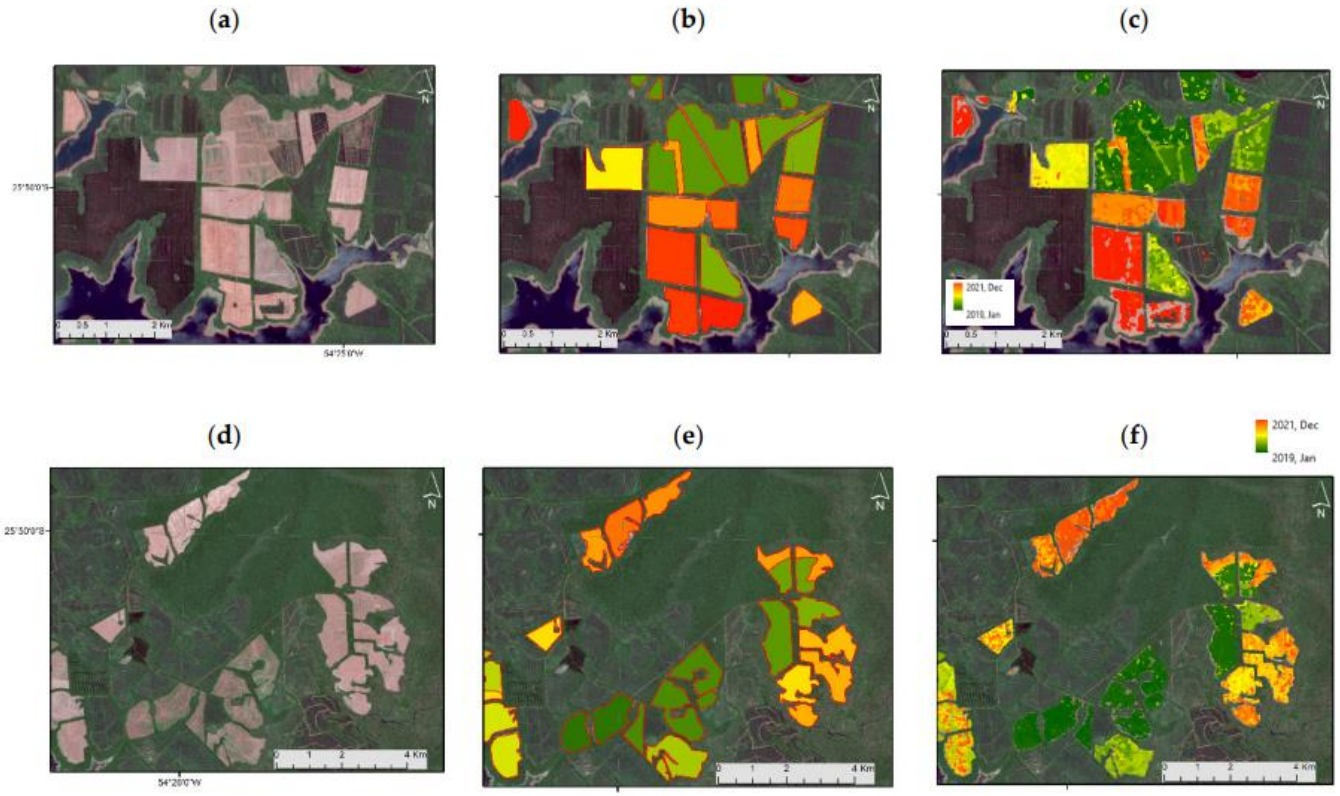

Figure 5. Reference data and colored pixels as a function of the estimated deforestation date for the two areas in Iguazu (shown as red rectangles in Figure 1). The first column (**a**,**d**) shows the multispectral Sentinel-2 image acquired in December 2021. The second column (**b**,**e**) shows the reference plots colored according to the reference date. The third column (**c**,**f**) shows the detected deforested pixels colored according to the estimated date. The color scale is linear and ranges from January 2019 (dark green) to December 2021 (dark red).

Detecting Deforestation Using Logistic Analysis and Sentinel-1 Multitemporal Backscatter Data

Adrian Dascălu [1], João Catalão [2,*] and Ana Navarro [2]

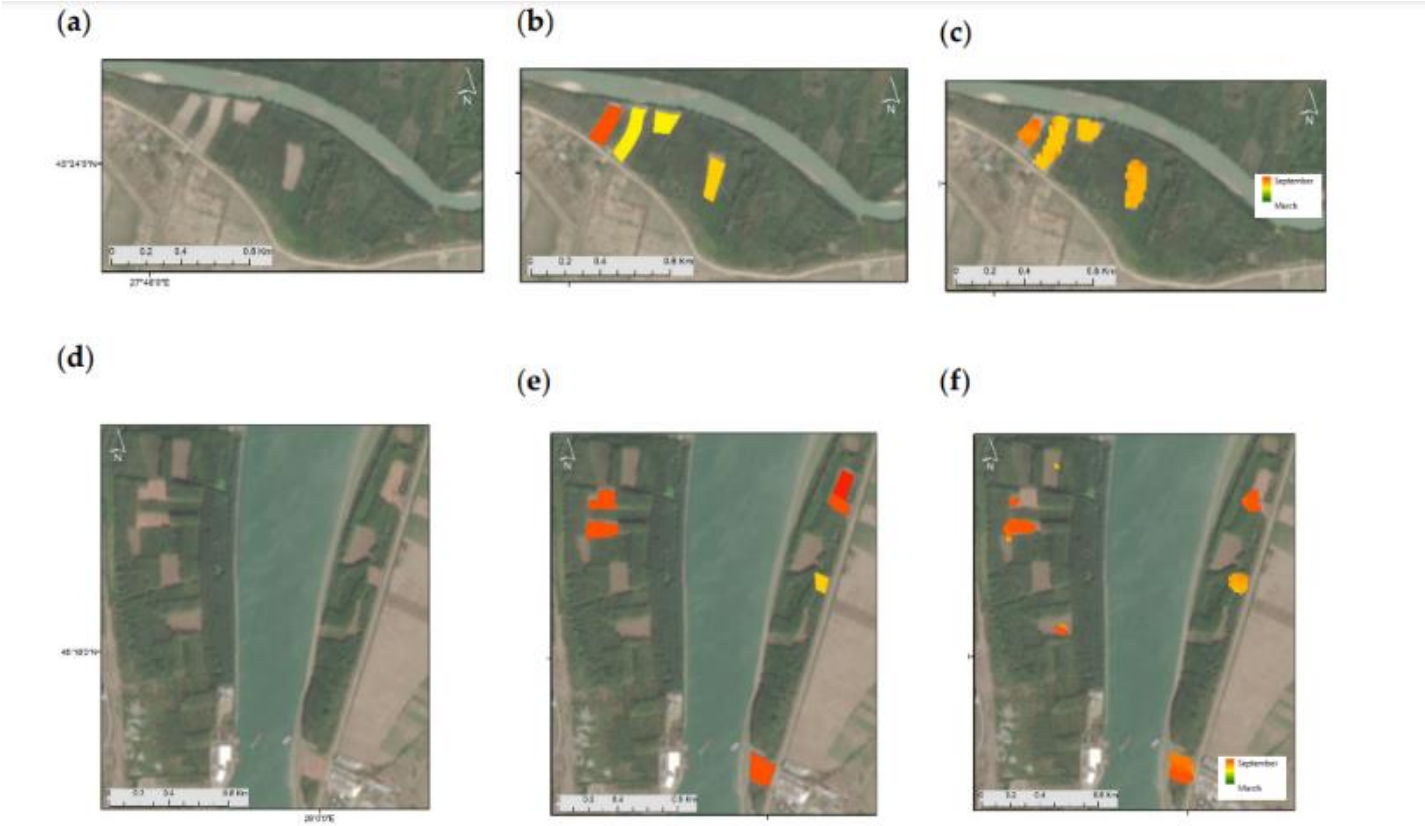

Figure 6. Reference data and colored pixels as a function of the estimated deforestation date for the two areas in Brăila (shown as red rectangles in Figure 1). The first column (**a**,**d**) shows the multispectral Sentinel-2 image acquired in September 2021. The second column (**b**,**e**) shows the reference plots colored according to the reference date. The third column (**c**,**f**) shows the detected deforested pixels colored according to the estimated date. The color scale is linear and ranges from January 2019 (dark green) to December 2021 (dark red).

Detecting Deforestation Using Logistic Analysis and Sentinel-1 Multitemporal Backscatter Data

Adrian Dascălu [1], João Catalão [2,*] and Ana Navarro [2]

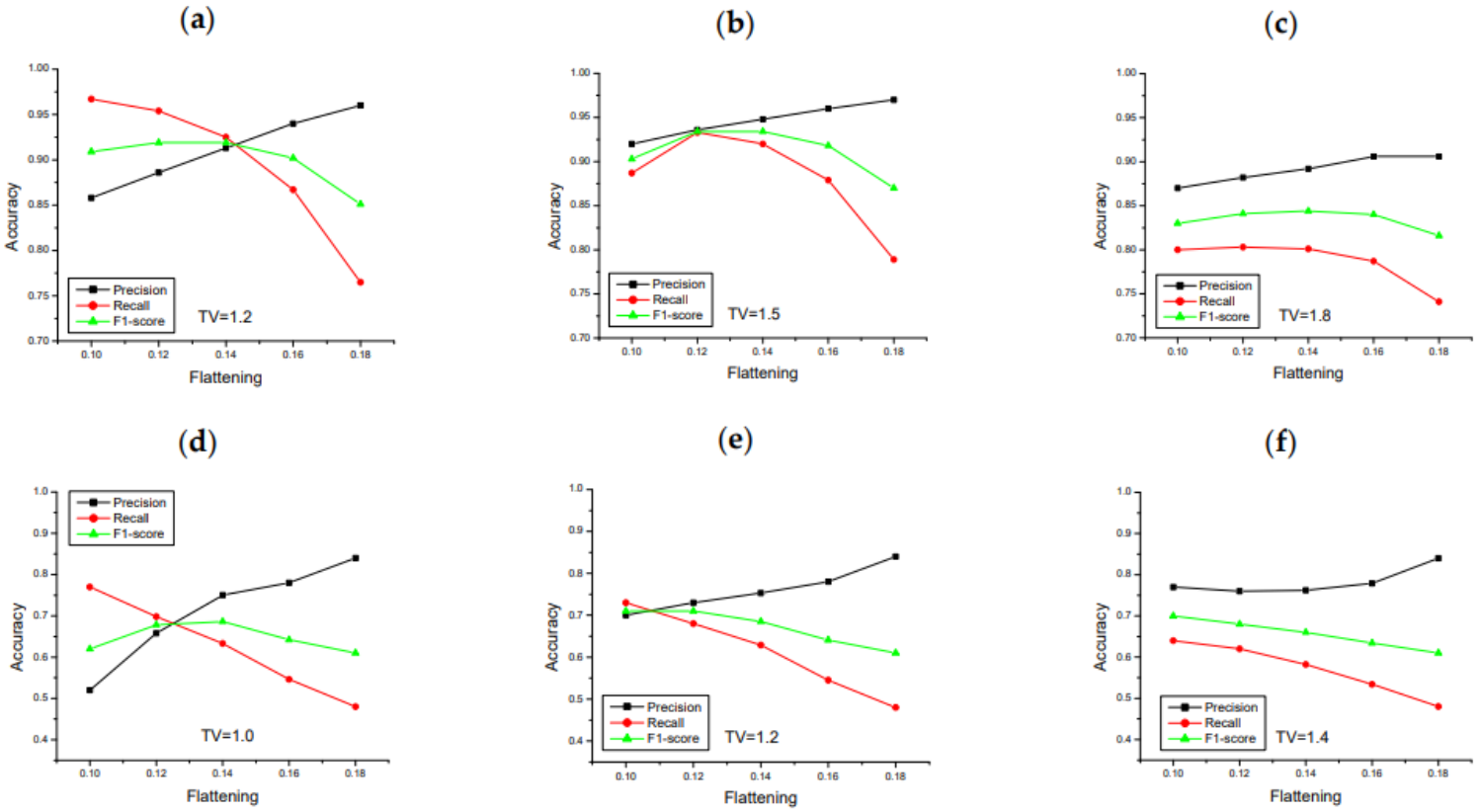

Figure 7. Deforestation detection accuracy as a function of the temporal variability and flattening. The first row shows the results for Iguazu with increasing temporal variability: (**a**) 1.2; (**b**) 1.5 and (**c**) 1.8. The second row shows the results for Brăila with increasing temporal variability: (**d**) 1.0; (**e**) 1.2 and (**f**) 1.4.

Ciências ULisboa

Ideas to develop / Challenges

1. Transfer learning in space and time
2. Unbalanced data classes (parcels)
3. Deep learning - CNN
4. Long short term memory (forecast)
5. Generative adversative Networks
6. Object recognition/segmentation